ECMWF COPERNICUS REPORT

Copernicus Atmosphere Monitoring Service

The Copernicus Atmosphere Monitoring Service global and regional emissions (April 2019 version)

Issued by: Laboratoire d'Aérologie / Claire Granier

Date: 20/05/2019

IMPLEMENTED BY ECMWF

The Copernicus Atmosphere Monitoring Service global and regional emissions (April 2019 version)

AUTHORS:
C. Granier (Laboratoire d'Aérologie, Toulouse, France and NOAA/ESRL/CSD-CIRES, University of Colorado), S. Darras (Observatoire Midi-Pyrénées), H. Denier van der Gon (TNO), J. Doubalova (Charles University), N. Elguindi (Laboratoire d'Aérologie), B. Galle (Chalmers University), M. Gauss (Norwegian Meteorological Institute), M. Guevara (Barcelona Supercomputing Center), J.-P. Jalkanen (Finnish Meteorological Institute), J. Kuenen (TNO), C. Liousse (Laboratoire d'Aérologie), B. Quack (GEOMAR Helmholtz-Zentrum für Ozeanforschung), D. Simpson (Norwegian Meteorological Institute), K. Sindelarova (Charles University)

CITATION:
Granier, C., S. Darras, H. Denier van der Gon, J. Doubalova, N. Elguindi, B. Galle, M. Gauss, M. Guevara, J.-P. Jalkanen, J. Kuenen, C. Liousse, B. Quack, D. Simpson, K. Sindelarova, The Copernicus Atmosphere Monitoring Service global and regional emissions (April 2019 version), Copernicus Atmosphere Monitoring Service (CAMS) report, 2019, doi:10.24380/d0bn-kx16.

Table of Contents

1. Introduction

In order to drive atmospheric models performing forecasts and analyses of air quality and atmospheric composition, an accurate quantification of surface emissions from anthropogenic and natural sources is required. As part of the European Copernicus Atmosphere Service (CAMS), diverse emission datasets have been developed. Global and regional European anthropogenic emissions for several sectors for a large number of atmospheric compounds have been developed. In addition, detailed emissions from ships based on ship identification systems have been developed. Different datasets providing natural emissions are being processed, such as the emissions of biogenic volatile organic compounds from vegetation, nitrogen compounds emissions from soils, emissions from the oceans and emissions from volcanoes. Methodologies for evaluating the emissions and their consistency at different scales are being generated. Temporal profiles at different scales are also being developed.

All the emissions developed in CAMS are available from the ECCAD (Emissions of atmospheric Compounds and Compilation of Ancillary Data (eccad.aeris-data.fr) database.

This document details the status of the development of each dataset in March 2019. Each of the datasets will be detailed in publications submitted in due course.

Until these publications are available for citations, we request that all users of the CAMS datasets discussed in this document cite this document, as well as the reference indicated for each dataset.

2. The CAMS regional anthropogenic emissions: CAMS-REG-AP and CAMS-REG-GHG

2.1 Methodology

The CAMS regional anthropogenic emission inventory covers emissions for UNECE-Europe for the main air pollutants and greenhouse gases. The method starts from the reported emissions by European countries to UNFCCC (for greenhouse gases) and to EMEP/CEIP (for air pollutants) and have been aggregated into 246 different combinations of sectors and fuels which were also the basis in the earlier TNO_MACC-II and TNO_MACC-III inventories (Kuenen et al., 2014). Because of the different level of detail in reporting between air pollutants and greenhouse gases, aggregation and/or disaggregation was performed to harmonize the sectors between all pollutants and countries.

2.1.1 Data collection

The reported data have been checked for gaps, errors and inconsistencies and form the basis for the CAMS regional inventory for 2000-2015 (CAMS-REG version 2.2) and 2016 (CAMS-REG version 3.1). Where needed, reported data from selected countries were replaced or completed using other emission data, most notably from:

- the IIASA GAINS model [http://gains.iiasa.ac.at/models/gains_models.html]
- the JRC EDGAR inventory [http://edgar.jrc.ec.europa.eu/]
- TNO bottom-up estimates for non-sea shipping

Expert judgement was used to assess the quality of each of these sources. Upon completion of an emission inventory for all countries, a consistent spatial distribution methodology is applied for Europe. For point sources information was collected on the location of power plants, large industrial installations, oil and gas production sites, airports and waste treatment locations (e.g. landfills). For area sources, proxies are collected which are thought to best represent the spatial variability of each specific emission source.

The spatial resolution of the emissions is 0.1° x 0.05° (lon x lat), in order to align with other emission inventories such as EDGAR and EMEP which have a resolution of 0.1° x 0.1° (lon x lat).
The sector classification has been changed from SNAP (used in the TNO-MACC inventory as well as in CAMS-REG-v1) to GNFR, as detailed in Table 2.1. GNFR is an aggregated version of the NFR (Nomenclature For Reporting) which is used by individual country emission reporting to EMEP and EU, and for consistency reasons it has also been implemented in the CAMS-REG emission inventory. More details on the sector classification can be found in in Table 2 and http://www.ceip.at/ms/ceip_home1/ceip_home/reporting_instructions/ .

GNFR_Category	GNFR_Category_Name	Link to SNAP
A	A_PublicPower	SNAP 1, only power and heat plants
B	B_Industry	SNAP 1 (non-power and heat plants) + SNAP 34 (or SNAP 3+4)
C	C_OtherStationaryComb	SNAP 2
D	D_Fugitives	SNAP 5
E	E_Solvents	SNAP 6
F	F_RoadTransport	SNAP 7
G	G_Shipping	SNAP 8, only shipping (all types)
H	H_Aviation	SNAP 8, only aviation
I	I_OffRoad	SNAP 8, non-shipping and non-aviation
J	J_Waste	SNAP 9
K	K_AgriLivestock	SNAP 10, livestock only
L	L_AgriOther	SNAP 10, non-livestock only
F1	F_RoadTransport_exhaust_gasoline	SNAP 71
F2	F_RoadTransport_exhaust_diesel	SNAP 72
F3	F_RoadTransport_exhaust_LPG_gas	SNAP 73
F4	F_RoadTransport_non-exhaust	SNAP 74 + SNAP 75 Note that SNAP 74 has only NMVOC and SNAP 75 has only PM emissions

Table 2.1: GNFR Sector explanation and link to SNAP nomenclature previously used in TNO-MACC-III and CAMS-REG version 1.

2.1.2 Spatial allocation of emissions

- For power plants, the locations and characteristics of each large power plant in Europe have been collected from the combination of various datasets:
    - E-PRTR (European Pollutant and Transfer Register, http://prtr.ec.europa.eu/)
    - CARMA database (Carbon Monitoring for Action, http://carma.org/)
    - Reporting of EU Member States to the Large Combustion Plants Directive
    - Platts-WEPP (World Electric Power Plants database, version December 2015, https://www.platts.com/products/world-electric-power-plants-database)

These datasets have been linked together to obtain a full overview of the power plants and to identify gaps and errors, which have been corrected and gap-filled to the extent possible.

- For industrial point sources, E-PRTR has been used. Absolute emissions have been obtained similar described above for power plants, for selected sectors and pollutants only.
- For both power plants and industrial sources, those emissions that could not be allocated to point sources (the difference between the national total that was reported and the sum of the point sources) has been spatially distributed using the industrial are land cover classification from CORINE.

- For population density, the default distribution for many sectors when no specific information is available, three versions of the Landscan population map (https://web.ornl.gov/sci/landscan/) (for the years 2005, 2010 and 2015) have been obtained. Urban and rural population maps have been created from the total population density map by comparing the population density in each cell (inhabitants/km^2).
- For airports, a new distribution map has been created based on Eurostat statistics on the passenger and freight flights by airport for all years 2000-2015, as well as airport locations (point sources). The main advantage of this update is that yearly specific maps can be created, reflecting the opening and closure of airports during the time series, as well as growth in air traffic in specific airports.
- For international shipping, the distribution is based on AIS data as described in Section 4. The ship emissions in CAMS-REG and CAMS-SHIP (see Section 4) have been harmonized: for example inland located ports like Rotterdam, Antwerp, Hamburg need to have a substantial contribution of international shipping emissions which will not automatically occur when using a sea area mask. This indicates the inherent difference between the division to sea/inland shipping and international/national navigation. The first will include emissions from ships travelling in sea regions, whereas the latter will describe the emissions occurring on inland waterways. In cases of Rotterdam and Hamburg, significant contribution comes from ships travelling on rivers flowing in or near these two cities. In the first approach these are counted as inland navigation, whereas they can be considered to fall into international navigation on the latter approach. In the past other distribution maps were used for on-sea emissions and separate in-port international shipping emissions were added and distributed using the size of the port as a scaling factor. This methodology is now replaced by the more realistic fully AIS-based approach for 2016. Scaling factors are developed for the shipping emissions to estimate emissions in the year 2000-2015 by sea, taking into account environmental control measures (Sulphur Emission Control Areas : SECA).

2.1.3 Emission profiles

In addition to the grid files, the following additional information is also provided:

- An updated PM speciation table is provided for 2000-2015 and 2016, distinguishing for both fine (<2.5µm) and coarse (2.5-10µm) particulate matter between EC, OC (represented as full mass, i.e. organic matter), sulphate, sodium and other minerals. A PM split is provided for each country and for each GNFR sector, so this split can be applied directly to the gridded emissions.
- An updated VOC speciation table is provided similar to the PM split for 2000-2015 and 2016, distinguishing over 20 different VOC compounds. This is provided also for each country and each GNFR sector in a table similar to the PM split table.
- Temporal profiles: default time profiles are provided per GNFR sector code (consisting of a variation between months, between days of the week and hours in the day).
- Effective emission height: a default effective height is provided per GNFR sector code.

2.2 Emissions data

Table 2.2 summarizes the characteristics of the CAMS-REG emissions for 2000-2015 (CAMS-REG-v2.2.1) and 2016 (CAMS-REG-v3.1). It should be noted that the two are not consistent since they are based on different reporting years, therefore methodology changes exist between the 2015 and the 2016 emissions which – in selected cases – could result in strong deviations between these two years.
Emissions for the following species are available: NO_x, SO_2, NMVOC, NH_3, CO, PM_{10}, $PM_{2.5}$, CH_4, from the CAMS-REG-AP dataset, and CO_2_ff (fossil fuel), CO_2_bf (biofuel), CH_4 from the CAMS-REG-GHG dataset. The emissions are provided as yearly averages, at a spatial resolution of 1/10° x 1/20° in longitude and latitude, i.e. about ~ 6x6 km over central Europe.
The domain covered by the dataset is: 30° W – 60° E and 30° N – 72°N.

CAMS-REG_v2.2.1 and v3.1 characteristics	
AP (Air Pollutants)	NO_x (as NO_2), SO_2, NMVOC, NH_3, CO, PM_{10}, $PM_{2.5}$, CH_4
GHG (Greenhouse Gases)	CO_2_ff (fossil fuel), CO_2_bf (biofuel), CH_4
Resolution	1/10° x 1/20° (longitude latitude, ~ 6x6 km over central Europe)
Period covered	2000-2015 (CAMS-REG-v2.2.1; annual emissions for each year) 2016 (CAMS-REG-v3.1; annual emissions)
Domain	30° W – 60° E 30° N – 72°N
Sector aggregation	GNFR (A to L), with GNFR F (Road Transport) split in F1 to F4 (total 16 sectors)
Emission unit	kg (both in CSV and NetCDF files)
Countries	42 countries + 13 sea regions *Note:* Emissions for other countries within the domain are added based on EDGAR v4.3.2

Table 2.2: Characteristics of the CAMS 2000-2015 regional European emissions (CAMS-REG_v2)

The emissions are given for different sectors, using the GNFR (Gridded Nomenclature For Reporting) sectorization. Table 2.3 gives the total emitted for the different compounds considered and for each country in the CAMS-REG domain for the year 2016 (CAMS-REG-v3.1). The names of the countries follow the ISO Aplha-3 codes for EU countries.

Country		NOX (as NO2)	SO2	NH3	NMVOC	CO	PM10	PM2_5	CH4	CO2_ff	CO2_bf
Original EU 15 countries plus Norway/Switzerland	AUT	143	14	68	115	563	31	18	263	67 401	23 672
	BEL	182	42	68	87	371	35	26	323	101 347	12 800
	CHE	59	6	57	71	162	17	7	197	38 230	6 169
	DEU	1 100	355	663	859	2 871	204	101	2 192	801 037	108 313
	DNK	78	10	75	67	241	31	20	286	37 043	17 223
	ESP	608	214	501	561	1 598	212	137	1 504	257 405	38 457
	FIN	116	40	31	72	302	33	20	190	47 491	39 839
	FRA	815	139	630	600	2 594	252	167	2 292	348 179	66 843
	GBR	808	166	289	703	1 498	170	107	2 088	393 050	37 591
	GRC	186	90	50	177	975	52	37	403	80 908	6 333
	IRL	73	14	117	67	108	29	16	551	39 606	2 248
	ITA	635	96	383	766	2 279	193	161	1 721	346 563	46 790
	LUX	12	1	6	9	17	2	1	25	5 240	521
	NLD	204	28	127	141	559	26	12	746	165 503	12 670
	NOR	113	15	28	141	377	35	26	197	41 589	5 222
	PRT	145	45	57	157	339	68	50	448	49 791	12 571
	SWE	112	19	53	136	417	38	18	192	41 755	31 889
New Member States	BGR	121	104	51	82	294	54	37	283	45 278	7 022
	CYP	15	16	6	8	15	2	1	34	7 299	205
	CZE	165	115	74	217	827	55	42	560	106 564	17 212
	EST	28	30	12	19	147	12	8	43	17 425	4 340
	HRV	48	15	36	65	225	28	21	178	18 160	6 495
	HUN	99	23	87	119	458	74	54	303	47 557	12 676
	LTU	45	16	35	47	172	16	9	134	13 157	6 145
	LVA	30	4	16	35	125	25	17	77	7 227	6 510
	MLT	4	2	1	3	3	1	0	8	1 333	26
	POL	677	582	268	613	2 542	263	149	1 844	320 826	34 255
	ROU	200	108	171	243	916	162	129	1 366	75 783	22 138
	SVK	61	27	31	60	244	34	27	176	34 041	6 856
	SVN	34	5	18	25	111	14	12	87	14 414	3 035
Non-EU countries	ALB	16	12	21	26	78	10	7	101	5 147	1 268
	ARM	29	178	21	54	227	36	25	122	14 879	3 830
	AZE	157	94	155	173	472	71	52	620	58 336	10 976
	BIH	9	48	5	5	121	1	1	24	2 958	48
	BLR	24	37	5	25	121	17	11	56	6 869	1 368
	GEO	15	4	16	30	115	17	13	86	6 306	1 790
	ISL	26	82	8	24	104	21	14	49	9 236	1 772
	MDA	7	7	2	12	52	5	4	20	1 929	669
	MKD	2 055	1 553	549	2 256	9 473	1 395	1 033	16 214	978 217	110 255
	RUS	81	309	49	100	485	87	56	204	43 829	5 704
	TUR	935	2 013	485	637	3 024	603	420	1 940	399 667	37 937
	UKR	624	1 030	278	491	3 362	593	417	3 144	298 961	27 624
	YUG	797	407	-	6	56	57	57	-	33 773	-
Sea regions	ATL	341	-	-	-	-	-	-	-	-	-
	BAS	149	-	-	-	-	-	-	-	-	-
	BLS	1 236	-	-	-	-	-	-	-	-	-
	MED	642	23	-	5	48	21	21	-	30 382	-
	NOS	32	708	-	14	119	110	110	-	77 492	-

Table 2.3: Total emissions by country and sea region for the year 2016 (Gg/yr)

2.3 Versions of the dataset

Two versions of the dataset are currently (March 2019) available:
- version 2.2 developed in August 2018, which gives the emissions for 2000-2015
- version 3.1, developed in March 2019, which gives the emissions for 2016

2.4 Contact

For information or questions on the CAMS regional anthropogenic emissions, contact:
- Jeroen Kuenen: jeroen.kuenen@tno.nl
- Hugo Denier van der Gon: hugo.deniervandergon@tno.nl

2.5 References

Kuenen, J. J. P., Visschedijk, A. J. H., Jozwicka, M., and Denier van der Gon, H. A. C.: TNO-MACC_II emission inventory; a multi-year (2003–2009) consistent high-resolution European emission inventory for air quality modelling, Atmos. Chem. Phys., 14, 10963-10976, https://doi.org/10.5194/acp-14-10963-2014, 2014.

3. The CAMS global anthropogenic emissions: CAMS-GLOB-ANT

3.1 Methodology

The CAMS global anthropogenic emissions are based on the emissions provided by the EDGARv4.3.2 inventory developed by the European Joint Center (JRC, Crippa et al., 2018) and the CEDS emissions (Hoesly et al., 2018) which provide emissions for the next IPCC report, AR6. Characteristics of these datasets are shown in Table 3.1.

Name of inventory	Species considered	Period covered	Spatial resolution
EDGARv4.3.2	BC, OC, NOx, NH3, SO2, NMVOCs, CO CO2, CH4 and N2O	1970-2012	0.1x0.1 degree
CEDSv3	BC, OC, NO_x, NH_3, SO_2, NMVOC, CO, CH_4, CO2	1850-2014	0.5x0.5 degree

Table 3.1: Characteristics used to develop the 2018 CAMS global emissions

Emissions for the period 2000-20189 emissions have been developed, using the following methodology:

- Use EDGARv4.3.2 emissions as a basis for 2010 emissions. EDGARv4.3.2 provides 0.1x0.1degree gridded emissions for different sectors on a monthly basis
- Calculate the trends in the emissions for 2011-2014 from the CEDS 0.5x0.5 degree emission dataset for each grid point.
- Disaggregate the trends to the same 0.1x0.1 degree grid as EDGARv4.3.2
- Merge and align sectors between the CEDS and EDGARv4.3.2 datasets, as discussed below
- Apply the 2011-2014 trends to the EDGAR4.3 2010 emissions to project emissions for the year 2018. Note that because we do not have data up to the year 2014 for the individual VOCs, a normalized trend calculated for NMVOCs is used to project the emissions for each of the twenty-five individual VOCS.
- Individual VOCs emissions are determined using the VOCs speciation provided by Huang et al. (ACP, 2017) and the JRC group.

Different sectors are available for the 2010-2019 emissions. Since the EDGAR v4.3.2 sectors and the CEDS sectors do not match, we defined the sectors for the CAMS global emissions to allow for the harmonization between the two datasets following Table 3.2. The CAMS global emissions are available for 11 sectors, as defined in the first column of the table. Note that these sectors have been created to roughly match the CAMS-REG-AG sectors in order to facilitate the merging of the two datasets in the future. In EDGAR, the sectors are not called the same way for reactive species, methane and VOCs: Table 3.2 shows the different names used in each inventory for each class of species. The names in parenthesis in the first column corresponds to the sector names in the NetCDF files that can be downloaded from ECCAD. For each sector, the 3rd column for the left shows which CEDS sector was used to determine the recent trends.

CAMS-GLOB-ANT sector	Species in CAMS-GLOB-ANT	CAMS-REG sector	IPCC Sector Name	IPCC Sector
Power Generation (ENE)	All species except VOCs	A_PublicPower	Energy Industry	1A1a
Power Generation (ENE)	All vocs		Power generation	1A1
Residential (RCO)	All species	C_OtherStationary Comb	Residential and other sectors	1A4
Road Transportation (TRO)	All species	F_RoadTransport	Road transportation	1A3b
Non-Road Transportation (TNR)	All species	I_OffRoad	Non-road ground transportation	1A3c__1A3e

Fugitive emissions from solid fuels (FEF)	All species except NH3, CO2_excl_sc, monoterpenes (11) and acids (24)	D_Fugitive	Fuel exploitation	1B1a_1B2a1_1B2a2_1B2a3_1B2a4_1B2c and 7A
Fugitive emissions from solid fuels (FEF)	All vocs except monoterpenes (11)		Manufacturing of solid fuels and fugitive emissions	
Industrial processes (IND)	All species except vocs	B_Industry	Oil refineries and transformation	1A1b_1A1c_1A5b1_1B1b_1B2a5_1B2a6_1B2b5_2C1b
Industrial processes (IND)	All species except CO2	B_Industry	Combustion in manufacturing industry	1A2
Industrial processes (IND)	All vocs		Industrial process and product use	2_3
Industrial processes (IND)	All species except NH3, OC and vocs	B_Industry	Iron and steel production	2C1a_2C1c_2C1d_2C1e_2C1f_2C2
Industrial processes (IND)	CO2, CO2_excl_sc, SO2, BC	B_Industry	Aluminum, magnesium and steel production	2C3_2C4_2C5
Industrial processes (IND)	All vocs except vocs monoterpenes (11), esters (18), ethers (19), chlorinated hydrocarbons (20), methanal (21), other alkanals (22), acids (24)		Petroleum refining and distribution	1A1b_1B2a5
Industrial processes (IND)	All species except CO2, OC, and vocs	B_Industry	Chemical processes	2B
Industrial processes (IND)	CO2, CO2_excl_sc	B_Industry	Non-energy use of fuel	2G
Industrial processes (IND)	NMVOC, CO2_excl_sc, NH3, SO2, BC, CO		Non-metallic mineral processes	2A
Industrial processes (IND)	NMVOC, NOx, SO2, BC, OC	B_Industry	Other production	2D
Solvents (SLV)	C02, NH3, NMVOC	E_Solvents	Solvents production and application	3
Agriculture (AGR)	NOx, NH3, CH4, CO, BC, OC and all vocs except alkanols (1), esters (18), chlorinated hydrocarbons (20), acids (24)	L_AgriOther	Agricultural waste burning	4F
Agriculture (AGR)	NOx, NH3, CH4, CO2	L_AgriOther	Agricultural soils	4C_4D1_4D2_4D4
Agriculture (AGR)	CH4	L_AgriOther	Enternic fermentation	4A
Manure Management (MMA)	NOx, NH3, CH4	K_AgriLivestock	Manure management	4B
Ships (SHP)	All species	G_Shipping	Ships	1A3d_1C2

Solid Waste and Waste Water (SWD)	All species except CO2_excl_sc and vocs	J_Waste	Waste incineration	6C
Solid Waste and Waste Water (SWD)	NH3, NMVOC, CH4	J_Waste	Solid waste disposal	6A_6D
Solid Waste and Waste Water (SWD)	NH3, NMVOC, CH4	J_Waste	Waste water	6B
Solid Waste and Waste Water (SWD)	All vocs except esters (18) and ethers (19)		Solid waste and waste water	6

Table 3.2: Details on the different sectors provided by the CAMS-AG emissions

Emissions for different VOCs are available in the CAMS global emissions, as indicated in Table 3.3. These emissions have been determined using the VOCs speciation provided by Huang et al. (ACP, 2017) and the JRC group. Table 3.3 shows the sectors for which emissions are provides for VOCs.

Name	Real name	ENE	RCO	TRO	TNR	FEF	SLV	AGR	SHP	SWD
voc1	Alcohols	X	X	X	X	X	X		X	X
voc2	Ethane	X	X	X	X	X	X	X	X	X
voc3	Propane	X	X	X	X	X	X	X	X	X
voc4	Butanes	X	X	X		X	X	X		X
voc5	Pentanes	X	X	X	X	X	X	X	X	X
voc6	Hexanes	X	X	X	X	X	X	X	X	X
voc7	Ethene	X	X	X	X	X	X	X	X	X
voc8	Propene	X	X	X	X	X	X	X	X	X
voc9	Ethyne	X	X	X	X	X	X	X	X	X
voc10	Isoprenes	X	X	X	X	X	X	X	X	X
voc11	Monoterpenes	X	X	X	X		X	X	X	X
voc12	Other alkad.	X	X	X	X	X	X	X	X	X
voc13	Benzene	X	X	X	X	X	X	X	X	X
voc14	Methylbenzene	X	X	X	X	X	X	X	X	X
voc15	Dimethylbenzenes	X	X	X	X	X	X	X	X	X
voc16	Trimethylbenzenes	X	X	X	X	X	X	X	X	
voc17	Other aromatics	X	X	X	X	X	X	X	X	X
voc18	Esters	X	X	X	X	X	X		X	X
voc19	Ethers	X	X	X	X	X	X	X	X	X
voc20	Chlorinated	X	X	X	X	X	X		X	
voc21	Methanal	X	X	X	X	X	X	X	X	X
voc22	Other alkanals	X	X	X	X	X	X	X	X	X
voc23	Alkanones	X	X	X	X	X	X	X	X	
voc24	Acids	X	X	X	X		X		X	X
voc25	Others	X	X	X	X	X	X	X	X	X

Table 3: List of VOCs considered in the inventory and corresponding sectors

3.2 Emissions data

Emissions for the following species are available: NO_x, SO_2, NH_3, CO, CO_2, CH_4, BC, OC, NMVOCs and 24 individuals VOCs.
The emissions are provided as monthly averages, at a 0.1x0.1 degree in latitude and longitude spatial resolution. An example of the emissions of CO for 2019 is shown in Figure 3.1 (left), and the changes in total emissions from 2000 to 2019 for NOx for a few sectors are shown in Figure 3.1 (right)

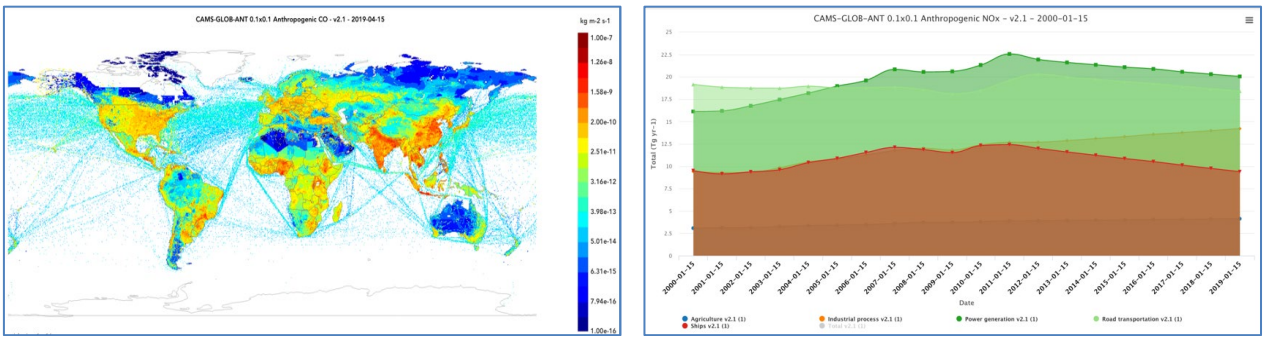

Figure 3.1: CO total emissions in April 2019 from the CAMS global inventory (left) and change in the NOx total emissions from different sectors from 2000 to 2019 from the CAMS global inventory (right)

3.3 Versions of the dataset

The current version of the 2000-2019 global anthropogenic emissions is called CAMS-GLOB-ANT_V2.1.

An analysis of satellite observations in China has shown that the tropospheric NO2 column has decreased in some regions of China since about 2012: such a feature is not shown in version 2.1 of CAMS-GLOB-ANT, which is based on datasets for the early 2010s. A group at the Tsinghua University in Beijing has developed recently emissions for more recent years for China, provided by the MEIC1.3 inventory. These emissions are available for the years 2008, 2010, 2012 and 2016. Another version of the CAMS-GLOB-ANT was developed, called CAMS-GLOB-ANT_v2.3: emissions are similar than in version CAMS-GLOB-ANT_v2.1, except for the emissions in China, which are replaced by emissions from MEIC 1.3.

3.4 Contact

For information or questions on the CAMS regional anthropogenic emissions, contact:
Nellie Elguindi: nellie.elguindi@aero.obs-mip.fr
Claire Granier: claire.granier@aero.obs-mip.fr
Sabine Darras: sabine.darras@obs-mip.fr

3.5 References

Crippa, M., Guizzardi, D., Muntean, M., Schaaf, E., Dentener, F., van Aardenne, J. A., Monni, S., Doering, U., Olivier, J. G. J., Pagliari, V., and Janssens-Maenhout, G.: Gridded emissions of air pollutants for the period 1970–2012 within EDGAR v4.3.2, Earth Syst. Sci. Data, 10, 1987-2013, https://doi.org/10.5194/essd-10-1987-2018, 2018.

Hoesly, R. M., Smith, S. J., Feng, L., Klimont, Z., Janssens-Maenhout, G., Pitkanen, T., Seibert, J. J., Vu, L., Andres, R. J., Bolt, R. M., Bond, T. C., Dawidowski, L., Kholod, N., Kurokawa, J.-I., Li, M., Liu, L., Lu, Z., Moura, M. C. P., O'Rourke, P. R., and Zhang, Q.: Historical (1750–2014) anthropogenic emissions of reactive gases and aerosols from the Community Emissions Data System (CEDS), Geosci. Model Dev., 11, 369-408, https://doi.org/10.5194/gmd-11-369-2018, 2018.

Huang, G., Brook, R., Crippa, M., Janssens-Maenhout, G., Schieberle, C., Dore, C., Guizzardi, D., Muntean, M., Schaaf, E., and Friedrich, R.: Speciation of anthropogenic emissions of non-methane volatile organic compounds: a global gridded data set for 1970–2012, Atmos. Chem. Phys., 17, 7683-7701, https://doi.org/10.5194/acp-17-7683-2017, 2017.

4. The CAMS ship emissions: CAMS-GLOB-SHIP

4.1 Methodology

Emissions originating from global shipping traffic were modelled using the Ship Traffic Emission Assessment Model (STEAM, Johansson et al., 2017; Jalkanen et al., 2016), which uses Automatic Identification System (AIS) data to describe ship traffic activity. Nowadays, all vessels larger than the 300 tons size limit globally report their position with a few second intervals; this has resulted in an availability of in-formation on ship activities at an unprecedented level of detail (Jalkanen et al., 2016). The ship emission inventories, which are based on such automated identification systems, have several significant advantages over the previously developed approaches. The CAMS ship inventory is therefore based on time-dependent, high-resolution dynamic traffic patterns, which can also allow for the effects of changing conditions, such as, e.g. marine and meteorological conditions (e.g. harsh winter conditions and sea ice cover) or weather routing.

The model output can be utilized in regional air quality models on an hourly basis and can also be used to assess the impacts of miscellaneous emission abatement scenarios (e.g., changes of fuel grade, the introduction of scrubbers and slow-steaming scenarios).

Vessel size growth and energy efficiency improvements have been taken into account as well as the introduction of IMO (International Maritime Organization) NOx Tiers when old vessels are replaced

by new ships. The main challenge for the global emission modelling of shipping is the treatment of the large number of vessels operating globally, for which it is difficult to obtain technical vessel specifications. To address this challenge, we propose a solution that includes the use of a web crawler and an algorithm that can be used to complete the missing technical details. Another issue is the sparsity of satellite based AIS-data which makes it necessary to analyse individual route segments and occasionally apply advanced route generation algorithms.
The same methodology is used for calculating the global and regions emissions from shipping: therefore, ship emissions for the European domain and ship emissions at the global scale are fully consistent. An example of the CO2 emitted from ships in 2016 is shown in Figure 4.1.

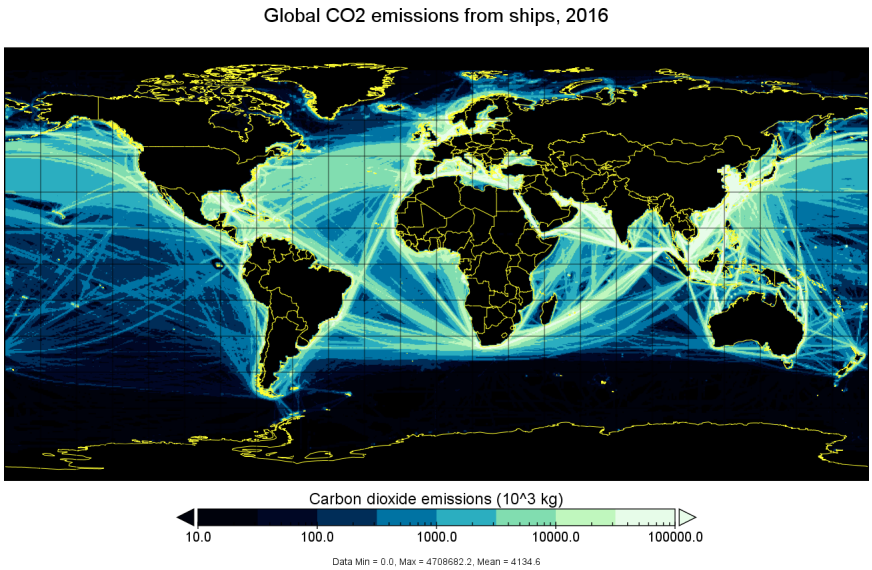

Figure 4.1: Global CO2 emissions from ships in 2016

The work to generate emission datasets for inland waterways is in progress.

4.2 Emissions data

Emission files are provided in NetCDF/CF conventions format and contain daily emission totals of NO_x, SO_x, CO, CO_2, VOC, EC, OC, Ash and SO_4. The last four species form the dry Particular Matter (PM) inventory, size range less than 2.5 micrometers. These files will be summed up and bee soon provided as monthly total emissions.
The emissions are available from 2000 to 2018 in the ECCAD database.
The emission data are available from the ECCAD database, as daily maps with 0.25 degree resolution. It should be noted that these data are for sea areas and do not include contributions from inland shipping. For inland shipping a separate data set will be produced for each of the years, and will be available soon.

4.3 Versions of the dataset

The current version of the 2000-2019 global anthropogenic emissions is called CAMS-GLOB-SHIP_v1.1.

4.4 Contact

For information or questions on the CAMS regional anthropogenic emissions, contact:
Jukka-Pekka Jalkanen (jukka-pekka.jalkanen@fmi.fi)

4.5 References

Jalkanen, J.-P., Johansson, L., and Kukkonen, J.: A comprehensive inventory of ship traffic exhaust emissions in the European sea areas in 2011, Atmos. Chem. Phys., 16, 71-84, https://doi.org/10.5194/acp-16-71-2016, 2016.

Johansson, L., J.-P. Jalkanen, and J. Kukkonen, Global assessment of shipping emissions in 2015 on a high spatial and temporal resolution, Atm. Env., 167, 403-415, doi: 10.1016/j.atmosenv.2017.08.042

5. The CAMS aircraft emissions: CAMS-GLOB-AIR

5.1 Methodology

Aircraft emissions are based on the CEDS aircraft emission data as described in Hoesly et al. (GMD, 2018). For the years up to 2014, the emissions are the same as CEDS. After 2014, we extrapolate in time using the trends calculated for the period 2012-2014. These dates were chosen because the trends are more stable after 2011, which may be a reflection of the global economic crisis.

For the speciation of VOCs, the emissions are based on the weights defined by EDGAR for landing and taking off (for the first two levels of the atmosphere corresponding to 0.305 km and 0.915 km), and for exhaust (corresponding to the rest of the levels up to 14.945 km). The emission for each individual VOC is calculated by multiplying these weights by the emissions for total VOCs.

5.2 Emissions data

Aircraft emissions are provided on a 0.5° X 0.5° horizontal grid for 25 levels, covering the period 2000-2019. An example of the NOx aircraft emissions in April 2019 at a 10km altitude is shown in Figure 5.1.

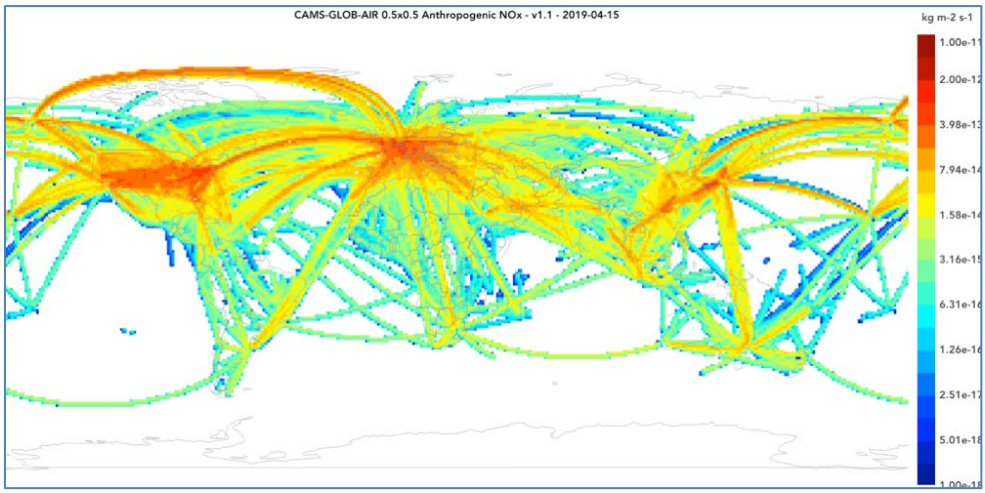

Figure 5.1: NOx emissions from aircraft at 10 km in April 2019.

5.3 Versions of the dataset

The current version of the 2000-2019 global anthropogenic emissions is called CAMS-GLOB-AIR_V1.1.

5.4 Contact

For information or questions on the CAMS global aircraft emissions, contact:
Nellie Elguindi: nellie.elguindi@aero.obs-mip.fr
Claire Granier: claire.granier@aero.obs-mip.fr
Sabine Darras: sabine.darras@obs-mip.fr

5.5 References

Hoesly, R. M., Smith, S. J., Feng, L., Klimont, Z., Janssens-Maenhout, G., Pitkanen, T., Seibert, J. J., Vu, L., Andres, R. J., Bolt, R. M., Bond, T. C., Dawidowski, L., Kholod, N., Kurokawa, J.-I., Li, M., Liu, L., Lu, Z., Moura, M. C. P., O'Rourke, P. R., and Zhang, Q.: Historical (1750–2014) anthropogenic emissions of reactive gases and aerosols from the Community Emissions Data System (CEDS), Geosci. Model Dev., 11, 369-408, https://doi.org/10.5194/gmd-11-369-2018, 2018.

6. The CAMS anthropogenic temporal profiles: CAMS-TEMPO

6.1 Methodology

The strategy to develop the CAMS emission temporal profiles consisted of: (i) assessing the most used temporal profiles for emission modelling, (ii) reviewing recognized and emerging state-of-the-art methodologies, (iii) collecting and analysing datasets linked to emissions variability, (iv) evaluating (when possible) the representativeness of the collected datasets for deriving reliable temporal emission profiles and (v) computing new temporal profiles using the knowledge acquired in the previous steps.

The datasets used as a benchmark for the development of the new temporal profiles, are:

- The TNO/TROTREP/POET profiles (Olivier et al., 2003)
- The GENEMIS project profiles (Friedrich and Reis, 2004)
- The LOTOS-EUROS profiles (Denier van der Gon et al., 2011)
- The EDGARv4 profiles (Janssens-Maenhout et al., 2017)
- The ECLIPSEv5 profiles (Klimont et al., 2017)

Figure 6.1 illustrates the profiles per pollutant sector reported in EDGAR (Janssens-Maenhout et al., 2017) and LOTOS EUROS (Denier van der Gon et al., 2011). The former is currently applied to the CAMS-GLOB_ANT emission inventory, and the latter was proposed for modelling purposes in the framework of the Monitoring Atmospheric Composition and Climate (MACC) project. In all cases, the profiles are assumed to be the same across all countries and independent of meteorology or different sociodemographic aspects. The only exceptions are the global profiles for the residential and agricultural sectors, which are approximated as a function of the geographical zone. Figure 6.1 illustrates the patterns for the northern hemisphere; they would be constant along the equator, and would be shifted by six months in the southern hemisphere.

In order to overcome the aforementioned limitations, the following features are considered in the CAMS emission temporal profiles:

- Pollutant-dependency: For some sectors, profiles were computed for all species independently in order to account for the variability of the activity patterns.
- Spatial variability: For almost all sectors, the temporal profiles are made country or even country and region-specific in order to take into account the effects of different sociodemographic patterns and climatology conditions, among other factors.
- Meteorological influence: For some sectors, the profiles were constructed using meteorological-dependent parametrizations (e.g. heating degree day concept) in order to account for the emissions variability driven by temperature or wind speed.

CAMS temporal profiles were developed for different sectors, including: energy industry, manufacturing industry, residential combustion, road transport and agriculture (fertilizer, livestock and agricultural waste burning). The following subsections describes the methods and information sources used to estimate the profiles for each sector.

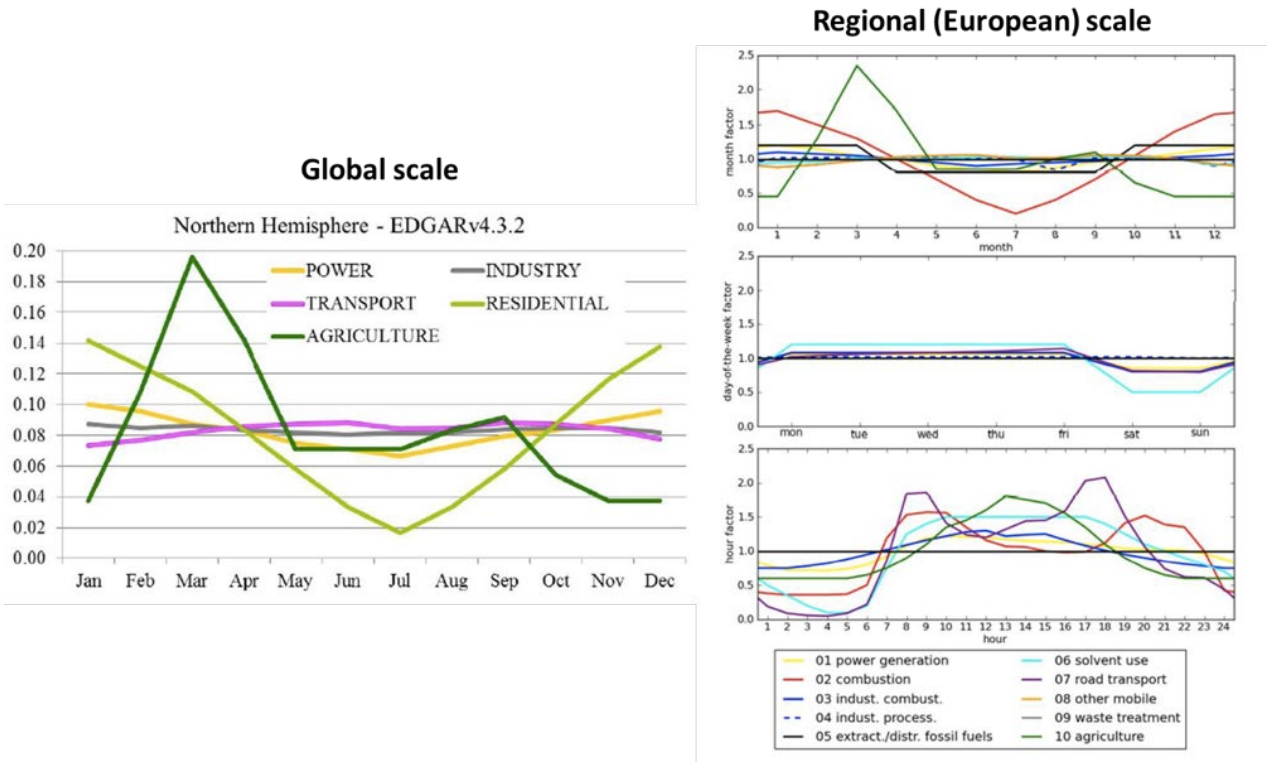

Figure 6.1: Monthly distribution of emissions used in EDGAR in the Northern Hemisphere (left) and monthly, weekly and diurnal profiles from LOTOS-EUROS (right)

6.1.1 Energy industry

The temporal variability of emissions from the industrial energy sector was estimated from national electricity production statistics after assuming that it depends to a large extent upon the combustion of fossil fuels in power and heat plants. This approximation is perfectly consistent with the definition of the GNFR sector "A_PublicPower" in the CAMS-REG_AP dataset, as it only includes emissions from these types of facilities. In the case of the CAMS-GLOB_ANT, the "ene" sector includes several other sources, but it is assumed that the profiles for power plants also apply to other types of facilities (e.g. refineries).

The dataset compiled to derive temporal profiles for this sector includes energy production data from multiple sources of information: the ENTSO-E Transparency Platform (Hirth et al., 2018; https://transparency.entsoe.eu/), the US EPA emission modelling platform (https://www.epa.gov/air-emissions-modelling), the Monthly Bulletin of Statistics (https://unstats.un.org/unsd/mbs/), and the IEA electricity statistics (http://www.iea.org/statistics/monthlystatistics/monthlyelectricitystatistics/)

For European countries and the US, monthly, weekly and diurnal pollutant-related profiles were derived using the ENTSO-E dataset and the US EPA emission modelling platform, respectively.

For other countries, pollutant-related monthly factors could not be developed since both the IEA and the MSB datasets do not report electricity production split by fuel. Hence, monthly factors were derived by averaging the available production data per month and relating them to the total production in the year. For countries with no information on hourly electricity production data, we assumed the diurnal profile reported under the MACC project for the SNAP01 sector.

6.1.2 Residential combustion

The temporal release of emissions from the residential combustion sector was assumed to be caused by the stationary combustion of fossil fuels in households and commercial buildings. These two source categories are assumed to be the main contributors to total emissions from the "Residential heating (res)" and the "C_OtherStationaryComb" sectors reported by the CAMS-GLOB_ANT and the CAMS-REG_AP/GHG inventories, respectively. Other combustion installations activities covered by these two sectors (i.e. plants in agriculture/forestry/aquaculture and other stationary) are assumed to follow the same temporal profile.

Gridded daily temporal profiles were derived according to the heating Degree Day (HDD) concept, which is an indicator used as a proxy variable to reflect the daily energy demand for heating a building (Quayle and Diaz, 1980). The profiles were developed for eight years (i.e. 2010 to 2017) using the daily mean 2m outdoor temperature reported by the ERA5 reanalysis dataset and considering a base temperature of 15.5 Celsius degrees a constant offset of 0.2 was also considered to account for those combustion processes not related to space heating but also to other activities that remain constant throughout the year such as water heating or cooking.

A profile based on the average of each day over all the available years was also produced. This profile should be used when performing emission modelling exercises for past or future years not included in the present dataset. Monthly gridded factors were also derived from the daily profiles for all the years available.

The diurnal behavior of residential combustion emissions varies according not only to the fuel but also the type of end-use (i.e. space heating or cooking). Subsequently, the following region and pollutant-dependent diurnal profiles are proposed:

- Developed countries:
    - For all pollutants except PM10, PM2.5, CO, CO2 and CH4 in urban/rural areas: use the MACC profile reported for SNAP02.
    - For PM10, PM2.5, CO, CO2 and CH4 in urban/rural areas: use an average of reported profiles linked to the combustion of residential wood (i.e. Finstad et al., 2004; Makkonen et al., 2011 and Athanasopoulou et al., 2017).

- Developing countries:
    - for all pollutants except PM10, PM2.5, CO, CO2 and CH4 in urban areas: use the MACC profile reported for SNAP02

- for PM10, PM2.5, CO, CO2 and CH4 in urban areas: use an average of reported profiles linked to the combustion of residential wood (i.e. Finstad et al., 2004; Makkonen et al., 2011 and Athanasopoulou et al., 2017).
- for all pollutants in rural areas, use profiles derived from measurements performed in households in the eastern Tibetan Plateau (Carter et al., 2016).

The assignation of the profiles was done under the following assumptions:

- PM10, PM2.5, CO, CO2 and CH4 emissions are mainly linked to wood combustion.
- In urban and rural areas of developed countries wood is mainly used for heating purposes.
- In urban areas of developing countries wood is mainly used for heating purposes.
- In rural areas of developing countries all fuels are used both for heating and/or cooking purposes (i.e. the two activities occur at the same time).

6.1.2 Manufacturing industry

The temporal variability of industrial emissions focuses on the manufacturing sector, as the contribution from these facilities dominates the total emissions. Both in the CAMS-GLOB_ANT and the CAMS-REG_AP/GHG inventories, all industrial emissions are reported under a single category (i.e. “Industrial processes (ind)” and “B_Industry”, respectively). Hence, the same temporal pattern has to be assumed for all types of facilities (e.g. cement plants, iron and steel plants).

Country-specific monthly profiles were estimated using the Industrial Production Index (IPI), which measures the monthly evolution of the productive activity of different industrial branches; that is, of the extractive, manufacturing, and production and distribution activities of electricity, water and gas. The IPI data was obtained from the MBS database (https://unstats.un.org/unsd/mbs/), which provides monthly information per country for the year 2015. For those countries without available information a flat profile is assumed. In the case of China, and due to its important contribution to total emissions, the monthly profile reported by the MIX inventory is assumed (Li et al., 2017). The time profiles were constructed based on IPI information from 2015 and it is assumed that they can be representative for other years.

Due to the lack of country-specific data, the weekly and diurnal temporal profiles provided in the framework of the MACC projects for SNAP03 sector are proposed.

6.1.3 Road transport

Road transport emissions reported by the CAMS global and regional inventories include exhaust (i.e. cold start and hot) and non-exhaust (i.e. gasoline evaporation and tyre/brake/road wear) sources. In CAMS-GLOB_ANT, all emissions are reported under a unique sector (i.e. road transport, “tro”), whereas in CAMS-REG_AP/GHG emissions are classified into four different categories (i.e. F1_RoadTransport_exhaust_gasoline, F2_RoadTransport_exhaust_diesel, F3_RoadTransport-exhaust_PG_gas and F4_RoadTransport_non-exhaust), the last one including both wear (PM10 and PM2.5) and evaporative emissions (NMVOC).

Considering this situation, it is assumed that the temporality of the CAMS-GLOB_ANT emissions is exclusively driven the traffic activity data. On the other hand, for the CAMS-REG_AP a distinction is made between exhaust/wear emissions and evaporative emissions. For the first group, temporal profiles were also developed based on traffic counts, whereas for the second one it was assumed that emissions are mainly affected by changes in ambient temperature.

In order to develop temporal profiles based on road transport activity, a compilation of traffic count data from multiple sources of information was performed. In most cases, information was obtained from local and national open data portals, whereas in other situations the data was collected from publications or through personal communications.

The results of the analysis highlight the importance of applying separate temporal profiles to characterize traffic and associated emissions for LDV and HDV. Nevertheless, in the present work this disaggregation was not considered since both the CAMS-GLOB_ANT and CAMS-REG_AP inventories report LDV and HDV-related emissions under the same pollutant sector.

The analysis of temporal patterns showed also that traffic regimes greatly vary not only according to the country but also to the region within a country (urban, rural). Therefore, country and region (urban, rural) specific monthly and weekly and diurnal profiles were constructed based on the compiled traffic information. In the case of the diurnal profiles, a separation between weekdays, Saturdays and Sundays is done. Urban and rural areas were defined according to the the Global Human Settlement Layer (GHSL) project (Pesaresi and Freire, 2016). For countries without any available temporal factors, assumptions were made considering geographical proximity.

The monthly profile constructed for NMVOC evaporative emissions is based on the emission results obtained using the High-Elective Resolution Modelling Emission System (HERMES) (Guevara et al., 2013). Summer and winter temperature dependent emission factors are defined for each type of vehicle as a function of the 2-m outdoor temperature, which is obtained from the ERA5 reanalysis. The HERMES model was run for the year 2016 at a spatial and temporal resolution of 4x4 km and 1 hour, respectively. The results were aggregated at the monthly level and normalized to derive temporal profiles.

The diurnal profile proposed for the NMVOC evaporative emissions is also based on the results obtained using the HERMES emission model. As in the case of the monthly profile, it is assumed that the diurnal variation is driven by changes in the outdoor temperature. HERMES computes for each grid cell and simulation day average 24-hour temperature profiles using the ERA5 reanalysis dataset. The resulting temporal pattern is constructed by averaging the profiles computed for all days and cells of the domain.

6.1.4 Agriculture

The CAMS global and regional emission inventories report the agricultural-related emissions in two separate sectors: “Agriculture (agr)” and “Agriculture livestock (mma)” (CAMS-GLOB_ANT) and

"K_AgriLivestock" and "L_AgriOther" (CAMS-REG_AP). In both cases, the first sector only includes emissions from livestock, whereas the second one reports emissions from several activities, mainly fertilizer applications and agricultural waste burning.

For the livestock sector, both in the global and regional inventories, it is assumed that NH3, NOx and NMVOC arise from the excreta of the animals and that they follow the same temporal pattern. The rest of pollutants are assumed to be a consequence of the animal activity (e.g. emissions of PM arise mainly from feed) and subsequently a flat profile is proposed for them.

For the "Agriculture (agr)" and "L_AgriOther" sectors, it is assumed that NH3 emissions are mainly related to fertilizer application, while the other pollutants (i.e. NOx, SOx, NMVOC, CO, PM10 and PM2.5) are dominated by agricultural waste burning. Hence, different temporal profiles are proposed for each group of pollutants.

The temporal distribution of NH3 emissions from fertilizer application depends mainly on the magnitude and timing of fertilizer application over different crop categories (i.e. planting schedule for each crop) and meteorological parameters that influence the volatilization of ammonia (i.e. temperature and wind speed) (Skjøth et al. 2011).

The proposed gridded monthly profile for this pollutant sector is based on the results estimated by the global bottom-up inventory of NH3 emissions (MASAGE_NH3) (Paulot et al., 2014) and the regional NH3 Chinese emission inventory reported by Zhang et al. (2018). MASAGE_NH3 provides information on the magnitude and seasonality of global NH3 emissions from individual crop and livestock sources on a 2.5 × 2.0 degrees grid, while the inventory of Zhang et al. (2018) reports total monthly NH3 emissions from fertilizer application and livestock in China at a resolution of 0.5 x 0.5 degrees. The CAMS gridded monthly profile is constructed as a combination of the MASSAGE_NH3 and the Zhang et al. (2018) inventories. The monthly weights derived from Zhang et al. (2018) were assigned to all those cells belonging to China, while for the other countries the MASSAGE_NH3-based profiles were applied. For sea cells a flat profile was assumed.

The temporal variation of emissions from livestock (i.e. manure management) are assumed to be dependent on temperature and ventilations rate or wind speed (Gyldenkærne et al., 2005). The specific parametrization varies as a function of the stage of the manure management practice (i.e. housing in open barns, housing in closed barns and storage). A gridded monthly profile is also constructed based on the results reported by the Paulot et al. (2014) and Zhang et al. (2018) emission inventories.

For the pollutants related to agricultural waste burning (e.g , NOx, SOx, NMVOC, CO, PM10 and PM2.5) the monthly gridded profiles reported by Klimont et al. (2016) under the ECLIPSE inventory are proposed. This temporal representation was developed based on the timing and location of active fires on agricultural land in the Global Fire Database (GFEDv3.1) (www.globalfiredata.org/Data/index.html) combined with annual emissions from the Greenhouse Gas and Air Pollution Interactions and Synergies (GAINS) model. All active grid cells in the monthly data from 1997 to 2010 in GFED were summed up and normalized.

Due to the lack of specific data, and following the profile reported under the MACC project for SNAP10 category, the weekly variation is assumed to be flat for all sectors (i.e. fertilizer application, livestock and agricultural waste burning) and pollutants.

Hourly NH3 emission rates from fertilizer application and livestock tend to vary with temperature, usually showing a peak in the middle of the day, when temperature peak. Due to the scarcity of data and the similarity observed between the profiles collected, it is proposed to maintain the profile used under the MACC project for sector SNAP10.

A new diurnal temporal profile for agricultural waste burning emissions is proposed based on the work by Mu et al. (2011), in which climatological mean diurnal cycles were constructed using GOES WF_ABBA active fire satellite observations from full hemisphere scans during 2007–2009. The reported profiles consist of eight 3-hourly fractions of emissions and vary as a function of vegetation type (i.e. forest, shrub/savanna and crop/grass) and region (e.g. Central America, Temperate North America). The proposed profile is based on the annual mean diurnal cycle constructed for the crop/grass category as an average of all regions.

6.2 Emissions data

The CAMS_TEMPO_v1.1 dataset consist on a collection of NetCDF and CSV files that report the constructed monthly, weekly/daily and diurnal temporal factors for each domain (global or regional), sector, pollutant and reference year. The NetCDF files are used to store the gridded profiles, while the CSV files report those profiles that are assumed to be constant across all countries and/or regions. In both cases, the sum of all factors is equal to 12 for monthly profiles, 7 for weekly profiles, 365 or 366 for daily profiles (depending if the reference year is leap or not) and 24 for diurnal profiles.

The spatial resolution of the global and regional NetCDF files are 0.1x0.1 degree and 0.1x0.05 degree, all of them following the same domain descriptions defined in the CAMS-GLOB_ANT and CAMS-REG_AP/GHG emission datasets, respectively.

The naming conventions for the global NetCDF files is as follows:

- CAMS-GLOB_Month_0.1x0.1_<sector>_<pollutant>_<year>_v1.1.nc
- CAMS-GLOB_Day_0.1x0.1_<sector>_<pollutant>_<year>_v1.1.nc
- CAMS-GLOB_Week_0.1x0.1_<sector>_<pollutant>_v1.1.nc
- CAMS-GLOB_Hour_0.1x0.1_<sector>_<pollutant>_v1.1.nc

Similarly, the regional NetCDF files are named as follows:

- CAMS-REG_Month_0.1x0.05_<sector>_<pollutant>_<year>_v1.1.nc
- CAMS-REG_Day_0.1x0.05_<sector>_<pollutant>_<year>_v1.1.nc
- CAMS-REG_Week_0.1x0.05_<sector>_<pollutant>_v1.1.nc
- CAMS-REG_Hour_0.1x0.05_<sector>_<pollutant>_v1.1.nc

The <sector> field follows the naming convention reported in the CAMS-GLOB_ANT and CAMS-REG_AP/GHG datasets. Note that the <pollutant> and <year> fields are only applied to those sectors in which the constructed profiles are pollutant and/or year dependent (e.g. the energy industry and residential combustion sectors, respectively).

6.3 Versions of the dataset

The current version of the CAMS temporal profiles is called CAMS_TEMPO_v1.1.

6.4 Contact

For information or questions on the CAMS temporal profiles, contact:
Marc Guevara: marc.guevara@bsc.es

6.5 References

Athanasopoulou, E., Speyer, O., Brunner, D., Vogel, H., Vogel, B., Mihalopoulos, N., and Gerasopoulos, E., Changes in domestic heating fuel use in Greece: effects on atmospheric chemistry and radiation, Atmos. Chem. Phys., 17, 10597-10618, https://doi.org/10.5194/acp-17-10597-2017, 2017.

Carter, E., Archer-Nicholls, S., Ni, K., Lai, A.M., Niu, H., Secrest, M.H., Sauer, S.M., Schauer, J.J., Ezzati, M., Wiedinmyer, C., Yang, X., Baumgartner, J., Seasonal and Diurnal Air Pollution from Residential Cooking and Space Heating in the Eastern Tibetan Plateau. Environ. Sci. Technol., 50 (15), 8353–8361, 2016.

Denier van der Gon, H.A.C., Hendriks, C., Kuenen, J., Segers, A., Visschedijk, A.J.H., Description of current temporal emission patterns and sensitivity of predicted AQ for temporal emission patterns. EU FP7 MACC deliverable report D_D-EMIS_1.3, 2011.

Finstad, A., Flugsrud, K., Haakonsen, G., Aasestad, K., Wood consumption, fire habits and particulate matter. Results from Folke and housing census 2001, Living Conditions Survey 2002 and Survey of wood consumption and firing habits in Oslo 2002Statistics Norway. Rapporter 2004/5 (in Norwegian), 2004.

Friedrich, R. and Reis, S. (Eds.), Emissions of Air Pollutants – Measurements, Calculation, Uncertainties – Results from the EUROTRAC-2 Subproject GENEMIS, Springer Publishers, Berlin, Heidelberg, Germany, 2004.

Guevara, M., Martínez, F., Arévalo, G., Gassó, S., and Baldasano, J.M., An improved system for modelling Spanish emissions: HERMESv2. 0. Atmos. Environ. 81,209–221, doi:10.1016/j.atmosenv.2013.08.053, 2013.

Gyldenkærne, S., Skjøth, C.A, Hertel, O., Ellermann, T., A dynamical ammonia emission parameterization for use in air pollution models, J. Geophys. Res., 110, D07108, doi:10.1029/2004JD005459, 2005.

Hirth, L., Mühlenpfordt, J., Bulkeley, M., The ENTSO-E Transparency Platform – A review of Europe's most ambitious electricity data platform, Applied Energy, 225, 1054-1067, 2018.

Janssens-Maenhout, G., Crippa, M., Guizzardi, D., Muntean, M., Schaaf, E., Dentener, F., Bergamaschi, P., Pagliari, V., Olivier, J. G. J., Peters, J. A. H. W., van Aardenne, J. A., Monni, S., Doering, U., and Petrescu, A. M. R., EDGAR v4.3.2 Global Atlas of the three major Greenhouse Gas Emissions for the period 1970–2012, Earth Syst. Sci. Data Discuss., https://doi.org/10.5194/essd-2017-79, 2017.

Klimont, Z., Kupiainen, K., Heyes, C., Purohit, P., Cofala, J., Rafaj, P., Borken-Kleefeld, J., and Schöpp, W., Global anthropogenic emissions of particulate matter including black carbon, Atmos. Chem. Phys., 17, 8681-8723, https://doi.org/10.5194/acp-17-8681-2017, 2017.

Li, M., Zhang, Q., Kurokawa, J.-I., Woo, J.-H., He, K., Lu, Z., Ohara, T., Song, Y., Streets, D. G., Carmichael, G. R., Cheng, Y., Hong, C., Huo, H., Jiang, X., Kang, S., Liu, F., Su, H., and Zheng, B., MIX: a mosaic Asian anthropogenic emission inventory under the international collaboration framework of the MICS-Asia and HTAP, Atmos. Chem. Phys., 17, 935-963, https://doi.org/10.5194/acp-17-935-2017, 2017.

Makonin, S.; Ellert, B.; Bajic, I.V.; Popowich, F., AMPds2-Almanac of Minutely Power dataset: Electricity, water, and natural gas consumption of a residential house in Canada from 2012 to 2014. Sci. Data, 3, doi:10.1038/sdata.2016.37, 2016.

Mu, M., Randerson, J. T., van der Werf, G. R., Giglio, L., Kasibhatla, P., Morton, D., Collatz, G. J., DeFries, R. S., Hyer, E. J., Prins, E. M., Griffith, D. W. T., Wunch, D., Toon, G. C., Sherlock, V., and Wennberg, P. O.: Daily and 3-hourly variability in global fire emissions and consequences for atmospheric model predictions of carbon monoxide, J. Geophys. Res.-Atmos., 116, D24303, doi: 10.1029/2011JD016245, 2010.

Paulot, F., Jacob, D. J., Pinder, R. W., Bash, J. O., Travis, K., and Henze, D. K.: Ammonia emissions in the United States, European Union, and China derived by high resolution inversion of ammonium wet deposition data: interpretation with a new agricultural emissions inventory (MASAGE_NH3), J. Geophys. Res.-Atmos., 119, 4343–4364, https://doi.org/10.1002/2013JD021130, 2014.

Quayle, R.G., Diaz, H.F., Heating degree day data applied to residential heating energy consumption. J. Appl. Meteorol. 19(3): 241–246, 1980.

Skjøth, C. A., Geels, C., Berge, H., Gyldenkærne, S., Fagerli, H., Ellermann, T., Frohn, L. M., Christensen, J., Hansen, K. M., Hansen, K., and Hertel, O., Spatial and temporal variations in ammonia emissions – a freely accessible model code for Europe, Atmos. Chem. Phys., 11, 5221-5236, https://doi.org/10.5194/acp-11-5221-2011, 2011.

Zhang, L., Chen, Y., Zhao, Y., Henze, D. K., Zhu, L., Song, Y., Paulot, F., Liu, X., Pan, Y., Lin, Y., and Huang, B.: Agricultural ammonia emissions in China: reconciling bottom-up and top-down estimates, Atmos. Chem. Phys., 18, 339-355, https://doi.org/10.5194/acp-18-339-2018, 2018.

7. The CAMS emissions of biogenic VOCs: CAMS-GLOB-BIO

7.1 Methodology

The emissions of VOCs from vegetation are calculated using the Model of Emissions of Gases and Aerosols from Nature (MEGANv2.10, Guenther et al., 2012), an emission model extensively used in the atmospheric modelling community for simulation of biogenic VOC emissions from vegetation and soils at regional and global scales. The MEGAN model was driven by ERA-Interim meteorological fields. Since emissions are being calculated on a monthly mean basis, synoptic monthly means of analyzed and forecasted parameters were retrieved from the ECMWF MARS server. These 3- or 6-hourly fields were interpolated in order to obtain monthly averaged daily profile of each meteorological variable.

The MEGAN model uses the following meteorological parameters: 2 m air temperature, 2 m dew point temperature, 10 m wind speed and surface pressure. The parameter photosynthetically active radiation (PAR) needed to drive MEGAN model is available in the ERA-Interim dataset, however it is calculated erroneously as documented in the Copernicus knowledge-base (see ECMWF Copernicus knowledge-base, ERA-Interim: surface photosynthetically active radiation (surface PAR) values are too low, https://confluence.ecmwf.int//display/CKB/ERA-Interim%3A+surface+photosynthetically+active+radiation+%28surface+PAR%29+values+are+too+low). As suggested by ECMWF, a surface downward solar radiation divided by a factor of 2.2 was used to approximate PAR.

The spatial distribution of vegetation in the MEGAN model is defined using plant functional types. This is an alternative approach to vegetation description using biomes (e.g. savanna, tundra). While biomes can consist of physiologically distinct vegetation types (e.g. grasses and trees), plant functional types group vegetation with similar leaf physiology, use of PFTs leads to less complex vegetation representation but allows physiologically-based ecosystem description convenient for the dynamic global vegetation models. The MEGAN model was designed to be coupled with the Community Land model (CLM4) and therefore uses the same approach, i.e. representation of the global land cover with 16 PFT categories (Lawrence and Chase, 2007). Vegetation in each model grid cell is defined by fractional coverage of each of the PFT. The list of PFTs used in the MEGAN model is presented in Table 7.1.

Emission factors for the main species (isoprene, main monoterpene species: α-pinene, β-pinene, 3Δ-carene, limonene, myrcene, sabinene and trans-β-ocimene, and MBO) are defined using gridded emission factor maps. These are available for download together with the MEGAN model code and are based on detailed land cover description and reflect regional information from measurement campaigns. For the rest of the modelled species each of the plant functional type (PFT) categories is assigned a species-specific emission factor and the final emission is calculated based on a fractional coverage of a grid cell by each PFT.

List of PFT categories

	Forest		*Herbaceous / Understorey*
1	Needleleaf Evergreen, Temperate	9	Broadleaf Evergreen Shrub, Temperate
2	Needleleaf Evergreen, Boreal	10	Broadleaf Deciduous Shrub, Temperate
3	Needleleaf Deciduous, Boreal	11	Broadleaf Deciduous Shrub, Boreal
4	Broadleaf Evergreen, Tropical	12	C3 Arctic Grass
5	Broadleaf Evergreen, Temperate	13	C3 Non-Arctic Grass
6	Broadleaf Deciduous, Tropical	14	Grass
7	Broadleaf Deciduous, Temperate	15	Crop
8	Broadleaf Deciduous, Boreal	16	Bare

Table 7.1. List of plant functional types (PFT) which are used in the MEGAN model to describe global vegetation coverage.

The vegetation seasonality is represented by changes in leaf area index (LAI). LAI is a dimensionless parameter defined as one-sided leaf area per area of the ground surface (m^2/m^2). Spatial and temporal distribution of LAI was obtained from processed observations of the MODIS instrument (Yuan et al., 2011). The 8-day observations were averaged to monthly means. Until today, only LAI data for the year 2016 are available. Therefore, for the 2017 model runs, a 10-year average LAI (2007-2016) for each month was calculated.

7.2 Emissions data

Global fields of gridded and speciated NMVOC emissions were calculated by the MEGAN model for the years 2000 – 2017. The mean global annual totals for the 2000-2017 period are given in Table 7.2. The main contributors to the NMVOC total are isoprene (64 %), monoterpenes (13 %), methanol (7 %), acetone (4 %), ethane (3.5 %), sesquiterpenes (2.5 %), propene (2.1 %), acetaldehyde (1.4 %) and ethanol (1.3 %). The rest of the species contributes each with less than 5 Tg(C)/year (i.e. 1 %). The mean annual total of emitted CO is 65 Tg(CO)/year. In Table 7.2, the totals estimated in the CAMS-GLOB-BIO inventory are compared to the previous MACC biogenic emissions inventory, MEGAN-MACC (Sindelarova et al., 2014).

species	**CAMS-GLOB-BIO.v1.1**	**MEGAN-MACC**	*molecular weight*
[Tg (species) / year]	*2000 - 2017*	*2000 - 2017*	*[g/mol]*
isoprene	385.5	594.2	68
α-pinene	25.7	32.7	136
β-pinene	14.1	16.9	136
other monoterpenes	38.8	46.9	136
methanol	99.7	130.2	32
acetone	32.5	37.9	58
acetaldehyde	13.6	19.1	44
formaldehyde	3.4	4.8	30
propane	0.03	0.03	44
propene	13.0	15.3	40
ethane	0.27	0.32	30
ethene	22.0	23.9	28
ethanol	13.6	19.1	46
sesquiterpenes	14.9	21.2	204
toluene	1.1	1.6	92
MBO	1.4	1.8	88
formic acid	2.5	3.6	46
acetic acid	2.5	3.6	60
butanes and higher alkanes	0.05	0.06	58
butenes and higher alkenes	2.6	3.1	56
other aldehydes	2.4	3.3	44
hydrogen cyanide	0.57	0.62	27
hydrogen sulfide	0.08	0.10	34
other ketones	0.6	0.7	72
total emissions			
Tg (C) / year	**532**	**765**	
CO	65.3	92.0	28

Table 7.1. List of modeled NMVOC species with annual global emission totals (Tg(species)/year) in CAMS-GLOB-BIO.v1.1 and MEGAN-MACC inventories averaged over the period of 2000 - 2017. Each species / group is assigned a molecular weight (right column) which was used to calculate total emissions in Tg (C) / year.

The emissions are available as monthly means and monthly averaged daily profiles. Horizontal spatial resolution of the data is 0.5 x 0.5 deg. The dataset is called CAMS-GLOB-BIO.v1.1, and provides emissions for 25 species and lumped species.

7.3 Versions of the dataset

The current version of the 2000-2017 global biogenic emissions is called CAMS-GLOB-BIO_V1.1.

7.4 Contact

For information or questions on the CAMS biogenic emissions, contact:
- Katerina Sindelarova: katerina.sindelarova@mff.cuni.cz
- Jana Doubalova: jana.doubalova@mff.cuni.cz

7.5 References

Guenther A.B., Jiang X., Heald C. L., Sakulyanontvittaya T., Duhl T., Emmons L. K., and Wang X. : The Model of Emissions of Gases and Aerosols from Nature version 2.1 (MEGAN2.1): an extended and updated framework for modeling biogenic emissions, Geoscientific Model Development, 5, 1471-1492, doi:10.5194/gmd-5-1471-2012, 2012

Lawrence, P. J. and Chase, T. N.: Representing a new MODIS consistent land surface in the Community Land Model (CLM 3.0), J. Geophys. Res. Biogeo., 112, G01023, doi:10.1029/2006JG000168, 2007.

Sindelarova, K., Granier, C., Bouarar, I., Guenther, A., Tilmes, S., Stavrakou, T., Müller, J.-F., Kuhn, U., Stefani, P., and Knorr, W.: Global dataset of biogenic VOC emissions calculated by the MEGAN model over the last 30 years, Atmos. Chem. Phys. Discuss., 14, 10725-10788, doi:10.5194/acpd-14-10725-2014, 2014.

8. The CAMS termite emissions: CAMS-GLOB-TERM

8.1 Methodology

Emissions of CH_4 from termite nests were estimated based on the methodology by Sanderson (1996). 11 ecosystems from the Olson vegetation database (Olson, 1989) were identified as termite habitats. As stated in Wood and Sands (1978), termites have been found up to 45°N and 45°S. Ecosystems falling outside these latitudes have therefore been excluded.

Each of the habitats was assigned termite biomass per m^2 and CH_4 emission flux per g of termite and hour (Table 8.1). Due to the diversity in termite species among the continents, different fluxes were considered for the regions of North and South America and Australia (group A) and for Europe, Africa and Asia (group B). Two of the habitats were also differentiated by humidity. Totals were then

calculated from the CH_4 flux per m^2 and these values were assumed to represent the annual total CH_4 emission per grid cell.

Habitat	Termite biomass [g/m²]	CH_4 flux [g CH_4/g/h]	
		group A	group B
Rain Green Forest	8	5.64	6.16
Tropical Rain Forest	11	5.64	6.16
Montane/Seasonal Forest	11.26	5.64	6.16
Temperate Forest	3	1.77	1.77
Savanna, Hot Grass - arid	0.96	2.9	7.6
Savanna, Hot Grass - nonarid	10.6	3.2	7
Succulent/Thorn - arid	0.98	2.9	7.6
Succulent/Thorn - nonarid	8.43	3.2	7
Farmland	5.38	3	3.9
Crops	2.25	3	3.9
Temperate Grass	5.2	1.77	1.77
Mediterranean, Eucalyptus, Acacia	5.3	4.13	4.13
Highland Scrub, Semidesert	2.7	4.13	4.13

Table 8.1. Termite habitats and their respective biomass and CH_4 fluxes

Jamali et al. (2011a) have found that CH_4 emissions from termite nests vary throughout the year due to seasonal changes in termite biomass and behaviour. These changes have mainly been correlated with moisture and temperature. We have used Global Precipitation Climatology Centre *(*GPCC; Schneider et al., 2011*)* precipitation data (long-term monthly means) to identify arid/nonarid regions and to introduce seasonality. Regions receiving less than 500 mm of precipitation per year were considered arid.

Seasonality was based on the study by Jamali et al. (2013) who measured and estimated monthly CH_4 fluxes from termites for a whole year. Monthly precipitation totals and temperature averages were fit with a linear regression model against the measurements made by Jamali et al. (2013) at Howard Springs, Australia (12.25°S, 131.25°E). Temperature was not statistically significant in the regression model, therefore the final model was based only on the precipitation data with a fit of R-squared 0.62. The annual emissions were distributed among the months of the year by the regression coefficients.

According to Anderson et al. (2010), Martius et al. (1996) and Kirschke et al. (2013), CH_4 emissions from termite nests do not significantly vary inter-annually and therefore our results are assumed to be representative for the whole period of 2000 - 2017, considered in the CAMS81 project.

8.2 Emissions data

The termites emissions dataset is gridded with a horizontal resolution of 0.5 x 0.5 degree. The emissions are given as monthly averages. The annual global emissions amount to 20.03 Tg(CH_4)/year, monthly totals are shown in Table 8.2.

Jan	Feb	Mar	Apr	May	Jun	Jul	Aug	Sep	Oct	Nov	Dec
1.75	1.67	1.8	1.64	1.59	1.57	1.78	1.84	1.63	1.56	1.53	1.67

Table 8.2. CH_4 emissions from termite nests - monthly global totals [Tg(CH_4)/month]

Most of the emissions are concentrated in the tropical regions within 15°N and 15°S with tropical Africa being the dominant source (Figure 8.1).

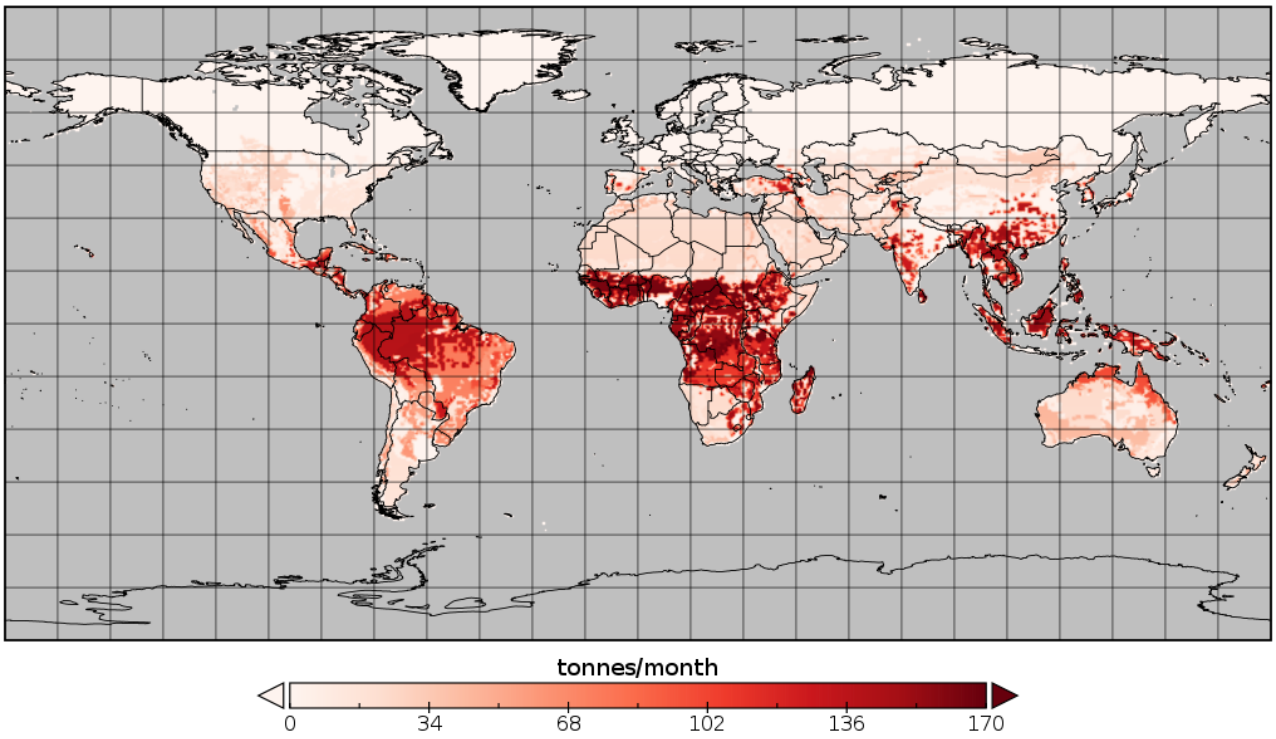

Figure 8.1: Spatial distribution of annual mean CH4 emissions from termites.

It is necessary to note that the estimate of the CH_4 emissions from termite nests is based on data and information with a very high level of uncertainty. The uncertainties originate mainly in the estimates of the representative termite biomass and CH_4 fluxes. These values were approximated by Sanderson (1996) from field measurements which may not be representative for all present

termite species. Also, Jamali et al. (2011b) reported a significant diurnal variation of CH_4 flux for several termite species. Flux measurements made at a single time during the day may lead to underestimated or overestimated values of the representative flux.

The emissions from termite nests however represent a relatively minor source from the global total CH_4 budget. According to Saunois et al. (2016), the total global emissions of CH_4 range from 540 to 884 Tg(CH_4)/yr. The total of 20.03 Tg(CH_4)/yr therefore represents only about 3 % of the global CH_4 emissions.

8.3 Versions of the dataset

The current version of the global methane emissions from termites is called CAMS-GLOB-TERM_V1.1.

8.4 Contact

For information or questions on the CAMS termites emissions, contact:
- Katerina Sindelarova : katerina.sindelarova@mff.cuni.cz
- Jana Doubalova : jana.doubalova@mff.cuni.cz

8.5 References

Anderson, B., Bartlett, K., Frolking, S., Hayhoe, K., Jenkins, J. and Salas, W., Methane and Nitrous Oxide Emissions from Natural Sources, Office of Atmospheric Programs, US EPA, EPA 430-R-10-001, Washington DC, 2010.

Jamali, H., Livesley, S. J., Dawes, T. Z., Hutley, L. B., Arndt, S. K., 2011a: Termite mound emissions of CH 4 and CO 2 are primarily determined by seasonal changes in termite biomass and behaviour. Oecologia (2011) 167:525–534, DOI 10.1007/s00442-011-1991-3.

Jamali, H., Livesley, S. J., Dawes, T. Z., Cook, G. D., Hutley, L. B., Arndt, S. K., 2011b: Dirunal and seasonal variations in CH_4 flux from termite mounds in tropical savannas of the Northern Territory, Australia. Agricultural and Forest Meteorology 151 (2011b), 1471-1479.

Jamali, H., Livesley, S. J., Grover, S. P., Dawes, T. Z., Hutley, L. B., Cook, G. D., Arndt, S. K., The Importance of Termites to the CH_4 Balance of a Tropical Savanna Woodland of Northern Australia. Ecosystems. DOI: 10.1007/s10021-011-9439-5, 2013.

Kirschke, S., et al., Three decades of global methane sources and sinks, Nat. Geosci., 6, 813–823, doi:10.1038/ngeo1955, 2013.

Martius, C., Fearnside, P.M., Bandeira, A.G., Wassman, R., Deforestation and methane release from termites in Amazonia, Chemosphere, 33, No. 3, p. 517-536, 1996.

Olson, J. S., Stanley, L., Colby, J., Ohrenschall, M., Olson World Ecosystems (WE1.4), NOAA/NGDC/WDC-A, Nat. Geophys. Data Cent., Boulder, Colorado, 1989.

Sanderson, M. G., 1996: Biomass of termites and their emission of methane and carbon dioxide: A global database. Global Biochemical Cycles, Vol. 10, No. 4, Pages 543-557, December 1996.

Saunois, M., Bousquet, P., Poulter, B., Ciais, P. et al., The global methane budget 2000–2012. Earth Syst. Sci. Data 8, 697–751, 2016.

Schneider, U., Becker, A., Finger, P., Meyer-Christoffer, A., Rudolf, B., Ziese, M., GPCC Full Data Reanalysis Version 6.0 at 0.5°: Monthly Land-Surface Precipitation from Rain-Gauges built on GTS-based and Historic Data. DOI: 10.5676/DWD_GPCC/FD_M_V7_050, 2011.

Wood, T. G., and Sands, W. A., The role of termites in ecosystems. Production Ecology of Ants and termites, edited by M. V. Brian, pp. 245-292, Cambridge Univ. Press, New York, 1978.

9. The CAMS soil emissions: CAMS-GLOB-SOIL

9.1 Methodology

For this first dataset, the basic methodology follows that of Yienger and Levy (1995) (hereafter YL95), with various updates to reflect recent literature and availability of data. Emissions are parameterized as a function of biome type, temperature and precipitation:

$$\mathrm{F}_{biome} = A'_{biome} \times f(T) \times g(\theta) \times \mathrm{F}_{pulse} \times \mathrm{CRF} \quad (1)$$

where F_{biome} is the soil NOx flux (ng(N) $m^{-2}s^{-1}$), A'_{biome} is a function of the biome-type, $f(T)$ is a function of temperature, $g(\theta)$ is a function of soil moisture, F_{pulse} is a function to account for pulsing of emissions, and CRF is the canopy reduction factor accounting for NOx-capture by the vegetation canopy above the soil. In YL95 A'_{biome} values were modified by estimates of locally available nitrogen (N_{avail}), which consists mainly of agricultural inputs of N (N from fertilizer, manure, hereafter N_{fert}), or atmospheric deposition of reactive nitrogen (hereafter N_{dep}). For this first estimate of emissions we prefer to calculate the contributions of N_{fert} and N_{dep}, separately, so we have:

$$\mathrm{F}_{soil} = \mathrm{F}_{biome} + \mathrm{F}_{N\,fert} + \mathrm{F}_{N\,dep} \quad (2)$$

Although Eqn. 1 implies that hourly calculations of soil emissions should be possible, given the availability of meteorological data, but we have aimed at monthly resolution for this study. One important reason is that many of the underlying data-sets have monthly resolution, and even this

has substantial uncertainties. Secondly, the most dramatic short-term variation with soil NO emissions is associated with pulses, and the estimation of the timing of such events cannot reliably be provided at this stage.

The calculations of F_{biome}, F_{Nfert} and F_{Ndep} are summarised in the next sections, as well as Pulsing (F_{pulse}) and canopy-reduction factors (CRF).

9.1.1 Calculation of F_{biome}

The biome emissions, F_{biome}, are driven by the underlying land-cover data, biome factors (A_{biome}), and meteorological drivers. Following YL95 and Steinkamp and Lawrence (2011), biome factors are given for dry and wet soils, with different temperature functions (f(T)) used for both. Biomes are here from the EMEP model's system which is a hybrid of the 'GLC-2000' land-cover data-set (http://bioval.jrc.ec.europa.eu/products/glc2000/glc2000.php), and the Community Land Model (http://www.cgd.ucar.edu/models/clm/, Oleson et al. 2010; Lawrence et al. 2011); details can be found in Simpson et al. (2017). Values of the emission factors were adapted from Steinkamp and Lawrence (2011) to the EMEP/CLM landcover categories. The ecosystem weighted factors are tabulated in Table 9.1.

Table 9.1: Biome-based emission factors (ng(N) m−2s−1) for dry and wet conditions. Biomes, mainly from CLM are mapped to the nearest category from Steinkamp and Lawrence 2011, denoted 'SL'.

Biome	Wet	Dry	SL category
NDLF EVGN TMPT TREE	1.66	12.18	18
NDLF EVGN BORL TREE	1.66	12.18	18
NDLF DECD BORL TREE	0.35	2.35	17
BDLF EVGN TROP TREE	0.44	2.47	20
BDLF EVGN TMPT TREE	0.36	2.39	15
BDLF DECD TROP TREE	0.08	0.62	19
BDLF DECD TMPT TREE	0.36	2.39	15,16
BDLF DECD BORL TREE	0.36	2.39	15,16
BDLF EVGN SHRB	0.84	6.18	9,10
BDLF DECD TMPT SHRB	0.09	0.65	6,7
BDLF DECD BORL SHRB	0.84	6.18	9,10
C3 ARCT GRSS	0.84	6.18	9,10
C3 NARC GRSS	0.42	3.07	12
C4 GRSS	0.42	3.07	12
Crop	0.44	2.47	20
Barren	0.06	0.43	5
Urban	0.57	0.0	22
Desert	0.0	0.0	
Water	0.0	0.0	0
Ice	0.0	0.0	2

Meteorological data are from the ECMWF IFS model, as processed for EMEP. These data had 3-hourly time resolution, and a 0.5°x0.5° degree longitude-latitude grid. As well as temperature, the most important meteorological input is soil water. The EMEP model uses a 'Soil moisture index' (SMI), taken from IFS, which is defined as:

$$\mathrm{SMI} = \frac{(\mathrm{SM\text{-}PWP})}{(\mathrm{FC\text{-}PWP})} \quad (3)$$

where SM is volumetric soil moisture, PWP is the permanent wilting point, and FC is the field capacity, all in $m^3\ m^{-3}$. SMI can be calculated in this way for each soil type in the grid, and then averaged to get a grid-average value which is more physically meaningful than a simple average over absolute volumetric soil moisture values. The SMI values used here from the upper 7 cm of the soil.

As seen from Table 1, we need to distinguish 'dry' from 'wet' soils. YL95 defined soils as being dry when the accumulated precipitation over the last 2 weeks was less than 1 cm, but subsequent authors have made use of NWP soil moisture data. Steinkamp and Lawrence (2011) defined the threshold between wet and dry soils at 15% volumetric soil moisture, which for an average soil was said to correspond to midway between PWP and FC, i.e. to SMI=0.5.

Soil temperatures (T_s) were estimated from air temperatures using simple empirical relationships, T_s (C) = T_a (C) + 5 for dry soils (following YL95) and T_s (K) = 0.72 T_a (K) + 82.28 for wet soils (algorithm from the code base of the MEGAN system, Guenther et al. 2012).

9.1.2 Calculation of F_{Nfert}

Global maps of global fertilizer and manure inputs were estimated by Potter et al. (2010, 2011), for the period of around 2000-2007. These data were converted to maps of N availability with 0..5°x0.5° degrees spatial resolution and monthly time resolution for the HEMCO system (Keller et al., 2014, http://wiki.seas.harvard.edu/geos-chem/index.php/HEMCO), as seen in Figure 9.3.

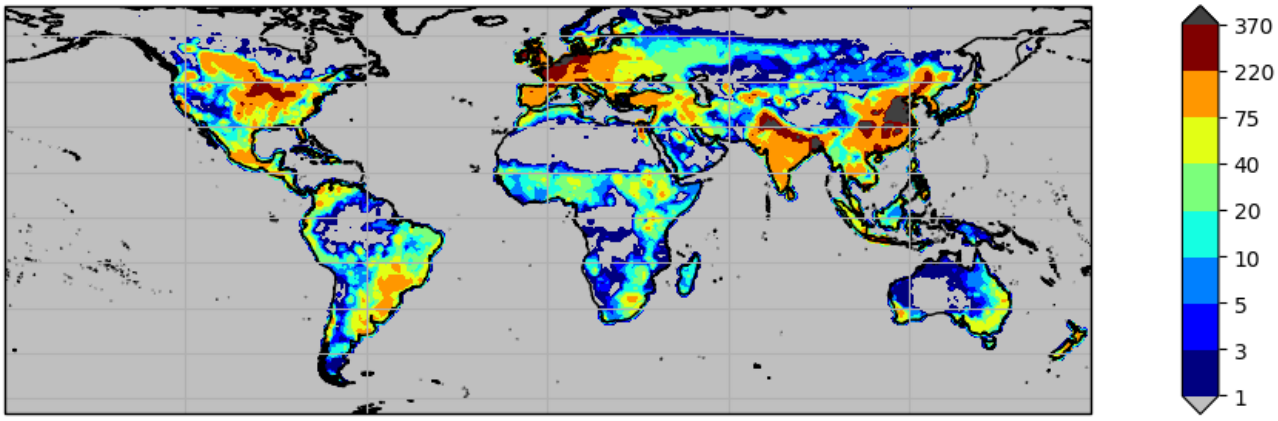

Figure 9.1: Inputs of fertilizer and manure (kgN/ha), from Potter et al. (2010), via HEMCO database.

These data were derived from N-inputs spanning the years 2000-2007, but with most emissions for the latter year (Potter et al., 2010). Hence we assigned these data a nominal year of 2005. Scaling

factors to get to other years were made by combining national year to year variations from the CEDS database (Hoesly et al., 2018) with global NH3 emission from ECLIPSEv5a database (www.iiasa.ac.at/web/home/research/researchPrograms/air/ECLIPSEv5a.html), with the latter needed to allocate country codes to grids. For this first emission estimate, where we only attempt monthly resolution of emissions, we adopted the simple procedure of allowing emission rates to follow these monthly N-inputs.
Potter et al. (2010) estimated N-inputs of 128.3 Tg(N) through manures and 70.2 Tg(N) through fertilizers, giving 198.5 Tg(N). Assuming 1% of this is released as soil NO emissions, we estimate a contribution of just under 2 Tg(N) for the base-year of 2005 in this work.

9.1.3 Calculation of F_{Ndep}

Estimates of atmospheric N-deposition were taken from the EMEP MSC-W chemical transport model (Simpson et al., 2012, 2014). Ideally we would have used global calculations at 0.5°x0.5° degrees resolution over the full 2000-2015 period, building upon the CAMS global emissions. However, such a CPU and time-intensive calculation was beyond the scope of this 1st deliverable, and so instead we have made use of more easily generated model calculations which provide the main trends in atmospheric N-deposition over this period. We have made use of model data for 2000, 2005, 2010 and 2014 from 1°x1° degree runs of the EMEP model. Emission data from ECLIPSEv5a interpolated back to 2000 and forward to 2014 using trends from the CEDS database (Hoesly et al., 2018). Data were linearly interpolated between these years and 2014 (the last year of CEDS data) were used for 2015. Given the large uncertainties in N-deposition, estimates (e.g. Simpson et al., 2014) this approach seemed acceptable for this first soil emissions calculation.

9.1.4 Calculation of F_{pulse}

Although many studies suggest that pulsing is important, and can in principle be calculated using precipitation (YL95) or soil water changes (e.g. Hudman et al., 2012), there is little evidence that such pulses can be accurately timed in global or even European scale CTMs. Indeed, Yan et al. (2005) noted that large scale NWP models have trouble predicting the conditions needed for pulsing, commenting that the ECMWF model's data never reached a value low enough to trigger a pulse in tropical savanna regions.
Tests conducted for this report showed that the timing of pulses varies greatly from one method to another (e.g. precipitation or SMI-based, and for different definitions of 'dry' versus 'wet'), so for this 1st delivery we simply set F_{pulse} = 1. Further work will be needed, for example based upon use of satellite soil moisture data and comparison to TROPOMI data, to find an algorithm which could be used with some confidence with regard to pulsing.

9.1.5 Calculation of CRF

It is well established that some of the NO emitted from soils can react quickly with ozone, forming NO2. Some of this NO2 is deposited within the canopy, reducing the emission of reactive N. YL95 used canopy reduction factors (CRFs) of between 0.25 for rain forests to 0.77 for Tundra, giving a global average of 0.53. These CRFs are very uncertain however, with Yan et al. (2005) estimating 0.67 and Hudman et al. (2012) found 0.84.

Given the uncertainties, and to partly compensate for the lack of pulsing emissions, we have elected to provide 'above-soil' estimates of soil NO emissions (ie CRF=1). Users may apply their own CRF values to this data-set.

9.2 Emissions data

Figure 9.2 illustrates the calculated soil NO emissions for the year 2010, giving total emissions and the three contributions from F_{biome}, F_{Nfert} and F_{Ndep}.. These plots illustrate the strong spatial variations in soil NO emissions, and also that the drivers vary markedly from region to region. For example, western European emissions are estimated to be strongly affected by the fertilizer-induced emissions, whereas in southern Africa or South America it is the biome component that strongly dominates. Atmospheric deposition is seen to be a relatively small contributor, but of course the relative contribution will increase away from agricultural source areas. Overall, year-to-year variations are not especially large, and trends are rather small.
Month to month variations in emissions are much more prominent. Seasonal cycles are driven largely by temperature and associated wet/dry changes. The large contribution of F_{Nfert} to Western European emissions is also very evident, with largest F_{Nfert} emissions near the start of the growing season.

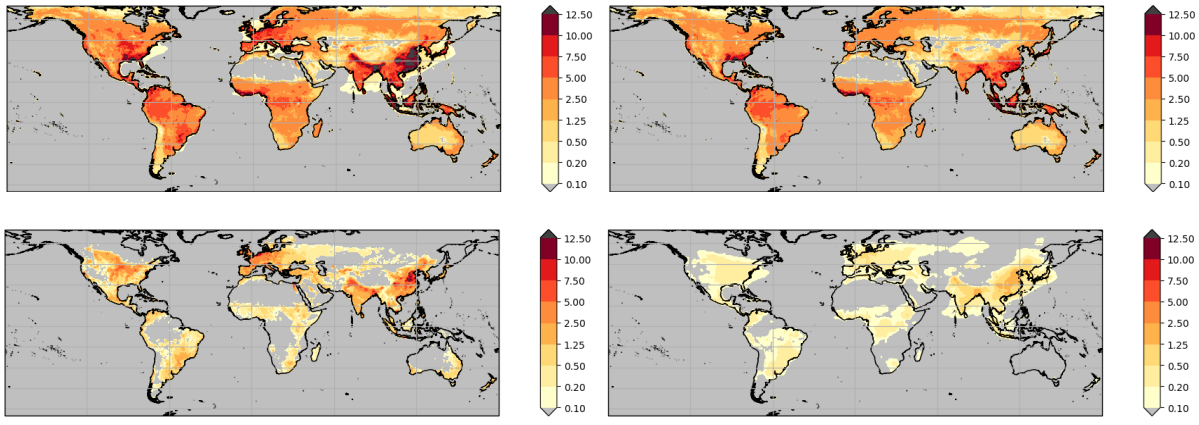

Figure 9.2: Above soil NO emissions (ng(N) m−2s−1) calculated for year 2010: (a) Total emissions, (b) Biome emissions (eqn 1), (c) Fertilizer-induced emissions (eqn 2), (d) Deposition-induced emissions (eqn 2)

Table 9.2 compares our estimates with other values from the literature. In general the global emissions fit rather well with literature values, including the recent satellite-derived estimate of Vinken et al. (2014). Emissions over Europe, North and South America are higher than those of Yan

et al. (2005), whereas results for Australia seem somewhat lower. The study of Simpson et al. (1999), although conducted in the 1990s, illustrated the large range of estimates possible from different methods. Unfortunately, no comparison was possible for Asia owing to unclear definitions of the regions (and the results shown for Europe also suffer from such ambiguities.). The data-set presented here is a first attempt at a multi-year soil NO emission estimate within CAMS-81. Estimation of such emissions is notoriously uncertain, since the emissions are driven by under-soil processes (microbial activity, pH, nutrients) rather than the simple meteorological and air quality variables which CTMs deal with.

Region	Emissions		
	Above soil [(a)]	Above canopy [(a)]	
Globe	12.92	(8.7)	This study
	12.9±3.9		Vinken et al., 2014
	10.7	(9.0)	Hudman et al. (2012)
	10.51	(8.61)	Steinkamp and Lawrence (2011)
	7.43	(4.97)	Yan et al. (2005)
		(8.9)	Jaeglé et al. (2005)
	10.2	(5.45)	Yienger and Levy (1995)
Europe	1.31	(0.88)	This study, EUR domain
	0.57	(0.38)	This study, WEUR domain
		(0.45)	Yan et al. (2005)
		(0.11-0.7)[b]	Simpson et al. (1999)
North America	2.17	(1.45)	This study
		(0.64)	Yan et al. (2005)
South America	2.26	1.51	This study
		(0.57)	Yan et al. (2005)
Australia	0.37	(0.25)	This study
		(0.46)7	Yan et al. (2005)

Table 2: Emissions of soil NO (Tg(N)/yr). Notes: (a) emissions from this study are average values over 2000-2015. The above canopy values are estimated for this table as 0.6 x 'Above soil', to be consistent with Yan et al. (2005). (b) range is from estimates using 'Skiba' and BEIS-2 methodologies as applied by Simpson et al. 1999. The YL95 estimate was presented there as 0.6 Tg(N)/yr.

We have here aimed at robustness rather than sophistication, in order to set up a transparent initial framework, and to avoid over-parameterising a model in which many of the underlying datasets (eg on agricultural inputs, or soil characteristics) are necessarily uncertain. Emissions have been provided on a monthly basis over the 2000-2015 period, since there seemed to be no basis for making estimates at shorted time duration that could be shown to be reliable.

Future revisions to this data-set will hopefully include a more detailed land-cover map, in which especially Savanna areas are delineated (the CLM-based map we currently use has rather generic grassland categories), improved estimation of soil temperatures, inclusion of the impact of forest-fires, and generally more use of satellite products to evaluate and constrain the estimated emissions.

Indeed, one important omission in this data-set is that of pulsing, where emission rates can be tens of times higher than base-rates with the onset of rain after a dry period. Defining 'dry' and thresholds for the amount of rain or soil moisture change has proven difficult though. A promising line of future work would be to make use of satellite data on surface soil moisture and NO measurements (TROPOMI) in areas where pulsing is expected, such as the Sahel in Africa. The various suggested algorithms for pulsing could then be tested in a systematic way, and implemented in future versions of the soil NO emission data-product.

9.3 Versions of the dataset

The global above soil (i.e., CRF = 1.0) emissions of NO are available, and his version is called CAMS-GLOB-SOIL_V1.1. Data are provided globally at 0.5◦×0.5◦degrees horizontal resolution for the 2000-2015 period, and with monthly time resolution. Emissions are provided as total values and also with separate data for soil NO emissions induced by fertilizers/manure and atmospheric deposition, so that users can provide their own modifications if wanted.

An important caveat is that this dataset is a first effort at CAMS soil NO emissions, and the methods need further evaluation and calibration. Note also that the user should provide their own CRF factors, which may depend on land-cover characteristics.

9.4 Contact

For information or questions on the CAMS soil emissions, contact:
David Simpson: david.simpson@met.no

9.5 References

Guenther, A. B., Jiang, X., Heald, C. L., Sakulyanontvittaya, T., Duhl, T., Emmons, L. K., and Wang, X.: The Model of Emissions of Gases and Aerosols from Nature version 2.1 (MEGAN2.1): an extended and updated framework for modeling biogenic emissions, Geoscientific Model Dev., 5, 1471–1492, doi: 10.5194/gmd-5-1471-2012, 2012.

Hoesly, R. M., Smith, S. J., Feng, L., Klimont, Z., Janssens-Maenhout, G., Pitkanen, T., Seibert, J. J., Vu, L., Andres, R. J., Bolt, R. M., Bond, T. C., Dawidowski, L., Kholod, N., Kurokawa, J.-I., Li, M., Liu, L., Lu, Z., Moura, M. C. P., O'Rourke, P. R., and Zhang, Q.: Historical (1750–2014) anthropogenic emissions of reactive gases and aerosols from the Community Emissions Data System (CEDS), Geoscientific Model Dev., 11, 369–408, doi:10.5194/gmd-11-369-2018, https://www.geosci-model-dev.net/11/369/2018/, 2018.

Hudman, R. C., Moore, N. E., Mebust, A. K., Martin, R. V., Russell, A. R., Valin, L. C., and Cohen, R. C.: Steps towards a mechanistic model of global soil nitric oxide emissions: implementation and space based-constraints, Atmos. Chem. Physics, 12, 7779–7795, doi:10.5194/acp-12-7779-2012, 2012.

Keller, C. A., Long, M. S., Yantosca, R. M., Da Silva, A. M., Pawson, S., and Jacob, D. J.: HEMCO v1.0: a versatile, ESMF-compliant component for calculating emissions in atmospheric models, Geoscientific Model Dev., 7, 1409–1417, doi:10.5194/gmd-7-1409-2014, 2014.

Lawrence, D. M., Oleson, K. W., Flanner, M. G., Thornton, P. E., Swenson, S. C., Lawrence, P. J., Zeng, X., Yang, Z.-L., Levis, S., Sakaguchi, K., Bonan, G. B., and Slater, A. G.: Parameterization Improvements and Functional and Structural Advances in Version 4 of the Community Land Model, J. Adv. Modeling Earth Systems, 3, doi:10.1029/2011MS000045, 2011.

Oleson, K., Lawrence, D., Bonan, G., Flanner, M., Kluzek, E., Lawrence, P., Levis, S., Swenson, S., Thornton, P., Dai, A., Decker, M., Dickinson, R., Feddema, J., Heald, C., Hoffman, F., Lamarque, J., Mahowald, N., Niu, G., Qian, T., Randerson, J., Running, S., Sakaguchi, K., Slater, A., Stockli, R., Wang, A., Yang, Z., Zeng, X., and Zeng, X.: Technical Description of version 4.0 of the Community Land Model (CLM), NCAR Technical Note NCAR/TN-478+STR, National Center for Atmospheric Research, National Center for Atmospheric Research, Boulder, CO, 2010.

Potter, P., Ramankutty, N., Bennett, E. M., and Donner, S. D.: Characterizing the Spatial Patterns of Global Fertilizer Application and Manure Production, Earth Interactions, 14, 1–22, http://dx.doi.org/10.1175/2009EI288.1, 2010.

Potter, P., Ramankutty, N., Bennett, E. M., and Donner, S. D.: Global Fertilizer and Manure, Version 1: Nitrogen Fertilizer Application, http://dx.doi.org/10.7927/H4Q81B0R, dataset, 2011.

Simpson, D., Winiwarter, W., Bo¨rjesson, G., Cinderby, S., Ferreiro, A., Guenther, A., Hewitt, C. N., Janson, R., Khalil, M. A. K., Owen, S., Pierce, T. E., Puxbaum, H., Shearer, M., Skiba, U., Steinbrecher, R., Tarraso´n, L., and O¨ quist, M. G.: Inventorying emissions from Nature in Europe, J. Geophys. Res., 104, 8113–8152, 1999.

Simpson, D., Benedictow, A., Berge, H., Bergstroem, R., Emberson, L. D., Fagerli, H., Flechard, C. R., Hayman, G. D., Gauss, M., Jonson, J. E., Jenkin, M. E., Ny´ıri, A., Richter, C., Semeena, V. S., Tsyro, S., Tuovinen, J.-P., Valdebenito, A., and Wind, P.: The EMEP MSC-W chemical transport model – technical description, Atmos. Chem. Physics, 12, 7825–7865, doi:10.5194/acp-12-7825-2012, http: //www.atmos-chem-phys.net/12/7825/2012/acp-12-7825-2012.html, 2012.

Simpson, D., Christensen, J., Engardt, M., Geels, C., Nyiri, A., Soares, J., Sofiev, M., Wind, P., , and Langner, J.: Impacts of climate and emission changes on nitrogen deposition in Europe: a multimodel study, Atmos. Chem. Physics, 14, 6995–7017, doi:10.5194/acp-14-0073-2014, http://www.atmos-chem-phys.net/14/0073/2014/acp-14-0073-2014.html, 2014.

Steinkamp, J. and Lawrence, M. G.: Improvement and evaluation of simulated global biogenic soil NO emissions in an AC-GCM, Atmospheric Chemistry and Physics, 11, 6063–6082, doi:10.5194/ acp-11-6063-2011, http://www.atmos-chem-phys.net/11/6063/2011/, 2011.

Vinken, G. C. M., Boersma, K. F., Maasakkers, J. D., Adon, M., and Martin, R. V.: Worldwide biogenic soil NO_x emissions inferred from OMI NO_2 observations, Atmospheric Chemistry and Physics, 14, 10 363–10 381, doi:10.5194/acp-14-10363-2014, https://www.atmos-chem-phys.net/14/10363/2014/, 2014.

Yan, X. Y., Ohara, T., and Akimoto, I.: Statistical modeling of global soil NOx emissions, Global Biogeochem. Cycles, 19, doi:10.1029/2004GB002276, 2005.

Yienger, J. and Levy, H.: Empirical model of global soil-biogenic NOx emissions, J. Geophys. Res., 100, 11 447–11 464, 1995.

10. The CAMS oceanic emissions: CAMS-GLOB-OCE

10.1 Methodology

Emissions for DMS, short-lived halogenated substances, and OCS from the oceans are given in the CAMS-GLOB-OCE dataset. Different methodologies have been used to derive the emissions for these three compounds or family of compounds.

10.1.1 DMS emissions

The calculation of DMS fluxes was performed using DMS concentrations in the ocean water. These concentrations were provided on 1°x1° spatial resolution by Lana et al., 2011. The data are derived from a large number of measurements performed during the 1980-2009 period and accessible from a web page of the Surface Ocean Lower Atmosphere Study (SOLAS), see https://www.bodc.ac.uk/solas_integration/implementation_products/group1/dms/. This site provides DMS concentration files on csv format, one file per month, in units of nmol(DMS)/L. The data are given as monthly means averaged over the period of measurements, but there is no inter-annual variation in the file. Hence, the concentrations are to be considered as average values representative of the 1989-2009 period.

The method to calculate DMS emissions also requires the u and v components of 10-meter wind speed as input. The Norwegian Meteorological Institute has run the ECMWF-IFS model to generate consistent data sets over multi-year time periods. Currently, global meteorological data are available to this project as netCDF files on 0.5°x0.5° spatial and 3-hourly temporal resolutions for

every year within the 1990-2017 period. Data for all these years have been generated with IFS version Cy40r1, except 2012 and 2013, which so far have been generated with Cy38r2 only. The differences between Cy38r2 and Cy40r1 (mainly related to cloud microphysics in the free troposphere) are much smaller than the uncertainty in other input parameters or the flux calculation itself. The multi-year meteorological data set can thus be considered as being consistent in the sense that it has been created by using essentially the same method/software for every year within the 2000-2015 period for which DMS emissions have been calculated.

The formulas to calculate ocean-atmosphere fluxes are based on equations by Nightingale et al. (2000) and their implementation in the Norwegian Earth System model. Within the frame of CAMS-81 these formulas have been implemented by MET Norway in a routine which reads all required input data, applies the formulas and writes the DMS emission data to netCDF files. The calculation proceeds as follows:

The 10-meter wind speed **U** is calculated from its u and v components as

U = sqrt (u^2+v^2) unit [m/s]

and the *gas exchange coefficient* k_{600} (for CO_2 in freshwater at 20°C) is calculated as

k_{600} = 0.222 * **U**^2 + 0.333 * **U** unit [cm/hr]

The flux of DMS is then calculated as

$F_{DMS} = k_{600}$*2.778e-15*M_{DMS}*C_{DMS} unit [kg(DMS)/m^2/s]

where M_{DMS} is the molecular weight of DMS (= 62.13 g/mol), C_{DMS} is the concentration of DMS in sea water [nmol(DMS)/L] and 2.778e-15 is a conversion factor to scale k_{600} to the gas exchange coefficient for DMS and to arrive at units of kg(DMS)/m^2/s.

Before writing out to the data files, the fluxes are averaged over one day. The sums are checked by multiplying fluxes with the areas of each grid cell, integrating over the globe.

In this first version of the emission data, daily means on a resolution of 0.5° x 0.5° resolution were calculated. This relatively high resolution does not reflect the (partly limited) accuracy of some of the input data, but it does correspond to the spatial resolution of the meteorological data and thus retains some of the high variability in wind speed, to which the gas exchange coefficient of DMS respond quite strongly (Nightingale et al., 2000).

10.1.2 Volatile short-lived halogenated substances

The calculation of halocarbon fluxes from the oceans are based on halocarbon concentrations in the ocean. These concentrations were provided on 1°x1° spatial resolution by Ziska et al. (2013). The data are derived from a large number of measurements, which were performed during the 1989-

2011 period. The data are accessible as supplementary material to the paper of Ziska et al. (2013) (at https://www.atmos-chem-phys.net/13/8915/2013/acp-13-8915-2013-supplement.zip). The zip-archive contains, inter alia, the text file Objective_Mapping_and_Linear_Regression_Data.txt, which was used to read in ocean and atmosphere concentrations of halocarbons, obtained through Objective Mapping and the Ordinary Least Square (OLS) technique. Ocean concentrations are given in units of pmol/L while atmospheric concentrations are given in parts per trillion by volume (pptv). There is no seasonal or inter-annual variation in the file, hence the concentrations are to be considered as average values representative of the 1989-2011 period.

The calculation of halocarbon fluxes also requires data on ocean water temperature, salinity and density. These data can be obtained from the World Ocean Atlas 2013, version 2, made available by NOAA at https://www.nodc.noaa.gov/OC5/woa13/woa13data.html. The data files, provided on netCDF format cover the period 1995 to 2012. The data are given as monthly means and are stored in two data sets: the first one is representative of the 1995-2004 period and features a spatial resolution of 1°x1°, while the second one is representative of the 2005-2012 period and is given on 0.25°x0.25° resolution. Temperature data are provided in degrees Celsius, density is given as sigma values (kg/m^3 in excess of 1000 kg/m^3), and salinity is given in practical salinity units (PSU, i.e. grams of salt per 1000 grams of sea water). In CAMS-81, the surface layer values of the 'objectively analyzed climatologies' (objectively interpolated mean fields for oceanographic variables at standard depth levels for the World Ocean) were used.

The method to calculate halocarbon emissions needs atmospheric pressure and 10-meter wind speeds (u_{10} and v_{10}) at the surface as input. The Norwegian Meteorological Institute has run the ECMWF-IFS model to generate consistent data sets over multi-year time periods. Currently, global meteorological data are available to this project as netCDF files on 0.5°x0.5° spatial and 3-hourly temporal resolutions for every year within the 1990-2017 period. Data for all these years have been generated with IFS version Cy40r1, except 2012 and 2013, which so far have been generated with Cy38r2 only. The multi-year meteorological data set can thus be considered as being consistent in the sense that it has been created by using essentially the same method/software for every year within the 2000-2015 period for which halocarbon emissions have been calculated.

The formulas to calculate ocean-atmosphere fluxes based on the input data described in the previous section were presented and explained by Ziska et al. (2013). Slightly updated versions were provided by Birgit Quack at GEOMAR. Within the frame of CAMS-81 these formulas have been implemented by MET Norway in a routine, which reads all required input data, applies the formulas and writes the halocarbon emission data to netCDF files.

The method proceeds as follows: After reading in the required input data the *diffusion coefficient* D, is calculated from the sea surface temperature for each halocarbon species separately (using different empirical coefficients). The *kinematic viscosity* v is calculated from the sea surface temperature, ocean water density, and ocean water salinity (parameters taken from the World Ocean Atlas). From the kinematic viscosity and diffusion coefficients the dimensionless *Schmidt Number SN* is calculated for each species separately. Using the *Schmidt number* as well as the 10-meter wind speed taken from ECMWF meteorological data we can calculate the *gas exchange coefficient* for each species. Furthermore, *Henry's law constant H* is calculated from the sea surface

temperature and empirically derived coefficients for each species separately. According to Henry solubility, the *equilibrium concentration* in sea water equals the *air concentration* of the species divided by Henry's law constant. The flux across the sea-air interface is finally calculated as the product between the gas exchange coefficient and the difference between the actual (measured) water concentration (from Ziska et al., 2013) and the equilibrium water concentration of the species in sea water.

Before writing out to the data files, the fluxes are averaged over one day and divided by 3600 to obtain units of pmol(species)/m^2/s. The sums are checked by multiplying fluxes with the areas of each grid cell, integrating over the globe, and comparing the results with numbers in Ziska et al. (2013).

10.1.3 OCS

The OCS emissions data set was compiled by S. Lennartz at GEOMAR (Helmholtz Centre for Ocean Research Kiel / Germany). It was provided to CAMS-81 in 2017 (S. Lennartz, pers. comm.) as a netCDF file containing OCS emissions on 2.8°x2.8° resolution (64 latitude bins and 128 latitude bins) in units of [g(S) m^{-2} $month^{-1}$]. Details on the data set are given in the publication of Lennartz et al. (2016) and supplementary material.

Lennartz et al. (2016) collected measurement data for the 2002 to 2014 period to create maps of OCS concentrations and used meteorological data from the ERA-Interim data set to calculate emission fluxes of direct and indirect sea-air fluxes of OCS. The original data file provided by S. Lennartz is called 'lennartz2017_ACP_OCSDMSCS2.nc' and contains direct emissions of OCS, but also indirect emissions in the form of short-lived DMS and CS_2 which are quickly oxidized into OCS.

10.2 Emissions data

10.2.1 DMS

Averaged over the 2000-2015 period, the annual global emissions of DMS calculated with the method and input data described above amounts to 35.7 Tg(S)/yr, which is within the uncertainty range of 24.1 to 40.4 Tg(S)/yr estimated by Lana et al. (2011). The emissions display a significant seasonal variation, with largest emissions during the summer season. Emissions are larger in the Southern Hemisphere than in the Northern Hemisphere.

Each of the files contains longitude values, latitude values, and the emissions of DMS from ocean water in units of kg(DMS)/m^2/s. In grid cells with no available data or over land, the emissions are set to zero. In grid cells containing both water and land surface, any non-zero flux value should only be applied to the fraction of the grid cell that is covered by ocean.

10.2.2 Volatile short-lived halogenated substances

In this first version of the emission data, we provide daily means on a resolution of 0.5° x 0.5° resolution. Obviously, this relatively high resolution does not reflect the (partly limited) accuracy of some of the input data, but it does correspond to the spatial resolution of the meteorological data and retains some of the high variability in surface pressure and 10-meter wind speeds, to which the fluxes responds quite strongly.

Averaged over the 2000-2015 period, the annual global emissions of the volatile short-lived halogenated substances CH_3I, CH_2Br_2 and $CHBr_3$ calculated with the method and input data described in Section 3 are, respectively, 1.39 Gmol(I), 0.93 Gmol(Br) and 2.37 Gmol(Br). This is slightly lower than, but still in quite good agreement with, the values obtained by Ziska et al. (2013). They get 1.45 Gmol(I)/year for CH_3I, 0.98 Gmol(Br)/year for CH_2Br_2, and 2.5 Gmol(Br)/year for $CHBr_3$ using the same method, with their input data, and the ordinary least squares regression technique.

Each of the files contains longitude values, latitude values, and the emissions of CH_3I, CH_2Br_2, and $CHBr_3$ from ocean water in units of pmol(species)/m^2/s. In grid cells with no available data or over land, the emissions are set to zero. In grid cells containing both water and land surface, any non-zero flux value should only be applied to the fraction of the grid cell that is covered by ocean.

10.2.3 OCS

The emissions show a clear seasonal variation in the emissions, with largest emissions during early summer. Negative emissions indicate uptake by the ocean. During winter months and, as described in Lennartz at al. (2016), also during night time, the ocean acts as a sink of atmospheric OCS. The total global annual direct emission of OCS in the file amounts to 139.6 Gg(S)/year (or 0.1396 Tg(S)/year). Lennartz et al. (2016) discuss the relatively high uncertainty range and suggest a total direct emission of 130±80 Gg(S)/year.

For CAMS-81 the data contained in lennartz2017_ACP_OCSDMSCS2.nc have been regridded to 1°x1° resolution, though without adding any fine-scale information. In addition to the regridding, the time dimension was modified and the field was translated by 180 degrees and flipped North-South, in order to get a similar format as the other data sets in the CAMS-GLOB-OCE inventory.

10.3 Versions of the dataset

The current version of the global soil emissions is called CAMS-GLOB-OCE_V1.1.

10.4 Contact

For information or questions on the CAMS oceanic emissions, contact:
Michael Gauss: michael.gauss@met.no

10.5 References

Lana, A., T. G. Bell, R. Simo, S. M. Vallina, J. Ballabrera-Poy, A. J. Kettle, J. Dachs, L. Bopp, E. S. Saltzman, J. Stefels, J. E. Johnson, and P. S. Liss, An updated climatology of surface dimethlysulfide concentrations and emission fluxes in the global ocean Global biogeochemical cycles 25, 17, 2011 doi.org/10.1029/2010GB003850, 2011.

Lennartz, S. T., C. A. Marandino, M. von Hobe, P. Cortes, B. Quack, R. Simo, D. Booge, A. Pozzer, T. Steinhoff, D. L. Arevalo-Martinez, C. Kloss, A. Bracher, R. Röttgers, E. Atlas, and K. Krüger Direct oceanic emissions unlikely to account for the missing source of atmospheric carbonyl sulfide Atmos. Chem. Phys. 17, 385–402, 2017 doi:10.5194/acp-17-385-2017.

Nightingale, P., G. Malin, C. Law, A. Watson, P. Liss, M. Liddicoat, J. Boutin, and R. Upstill-Goddard In situ evaluation of air-sea gas exchange parameterizations using novel conservative and volatile tracers Global biogeochemical cycles 14, 373-387, 2000 doi.org/10.1029/1999GB900091, 2000.

Ziska, F., Quack, B., Abrahamsson, K., Archer, S. D., Atlas, E., Bell, T., Butler, J. H., Carpenter, L. J., Jones, C. E., Harris, N. R. P., Hepach, H., Heumann, K. G., Hughes, C., Kuss, J., Krüger, K., Liss, P., Moore, R. M., Orlikowska, A., Raimund, S., Reeves, C. E., Reifenhäuser, W., Robinson, A. D., Schall, C., Tanhua, T., Tegtmeier, S., Turner, S., Wang, L., Wallace, D., Williams, J., Yamamoto, H., Yvon-Lewis, S., and Yokouchi, Y. Global sea-to-air flux climatology for bromoform, dibromomethane and methyl iodide Atmos. Chem. Phys. 13, 8915-8934, 2013 doi.org/10.5194/acp-13-8915-2013, 2013.
.

11. The CAMS volcanic emissions: CAMS-GLOB-VOLC

11.1 Methodology

The volcanic gas emission data are obtained from the NOVAC (Network for Observation of Volcanic and Atmospheric Change) network. For each volcano, data from one or several NOVAC Scanning mini-DOAS instruments are combined with meteorological information to derive daily statistics of total SO_2 emission from the volcano. The gas emission is calculated using the ScanDOAS technique described in Galle et al. (2010).

Analyzed wind data from ECMWF ERA-interim database were used, with a resolution of 0.125x0.125 deg, 6 h time resolution and up to 60 vertical levels from ground up to 0.1 hPa. Data is interpolated to the location of the volcanic vent and time of measurement for each flux calculation. Typically 1 – 3 instruments are installed on each volcano in order to cover different wind directions and facilitate plume height estimate. About 50 individual measurements are made by each instrument each day. Data from the different instruments are combined and if certain quality parameters are fulfilled a valid measurement results. Only daytime measurements are possible as

the method uses sky light for the measurement. For days having 5 or more valid measurements an average emission and standard deviation is calculated.

11.2 Emissions data

Emissions of SO2 for 20 volcanoes are provided from 2005 to 2010: only 16 showed significant emissions during the actual period. The investigated volcanoes are listed in Table 11.1.

Volcano	Country	Average SO_2 emission 2005 – 2010 [kg/s]
Arenal	Costa Rica	1.5
Etna	Italy	37.7
Concepción	Nicaragua	5.8
Fuego	Guatemala	3.3
Galeras	Colombia	11.7
Masaya	Nicaragua	4.2
Nevado de Ruiz	Colombia	1.0
Nyiragongo	D. R. Congo	14.7
Popocatépetl	Mexico	21.0
Santa Ana	El Salvador	2.0
San Cristóbal	Nicaragua	8.3
Telica	Nicaragua	1.9
Santiaguito	Guatemala	3.1
Tungurahua	Ecuador	20.1
Turrialba	Costa Rica	4.8
Vulcano	Italy	0.2
Santa Ana	El Salvador	0
Fuego de Guatemala	Guatemala	NA
Cotopaxi	Ecuador	0
Nyamulagira	D.R. Congo	NA

Table 11.1: Emissions for the 2005-2010 for different volcanoes.
NA: Not applicable due to lack of measurements during the period

11.3 Versions of the dataset

The current version of the global soil emissions is called CAMS-GLOB-VOLC_V1.1.

11.4 References

Galle, B., Johansson, M., Rivera, C., Zhang, Y., Kihlman, M., Kern, C., Lehmann, T., Platt, U., Arellano, S. and Hidalgo S., Network for Observation of Volcanic and Atmospheric Change (NOVAC) —A global network for volcanic gas monitoring: Network layout and instrument description, J. Geophys. Res., 115, D05304, doi:10.1029/2009JD011823, 2010.

Copernicus Atmosphere Monitoring Service

ECMWF - Shinfield Park, Reading RG2 9AX, UK

Contact: info@copernicus-atmosphere.eu